GRADUATE SCHOOL
EAST TENNESSEE STATE UNIVERSITY

East Tennessee State University
Digital Commons @ East Tennessee State University

Electronic Theses and Dissertations | Student Works

12-2021

Study of the Cell Membrane and the Synthesis of Chimeric Human Bacterial Phospholipids

Opeyemi O. Tade
East Tennessee State University

Follow this and additional works at: https://dc.etsu.edu/etd

 Part of the Organic Chemistry Commons

Recommended Citation

Tade, Opeyemi O., "Study of the Cell Membrane and the Synthesis of Chimeric Human Bacterial Phospholipids" (2021). *Electronic Theses and Dissertations*. Paper 3990. https://dc.etsu.edu/etd/3990

This Thesis - unrestricted is brought to you for free and open access by the Student Works at Digital Commons @ East Tennessee State University. It has been accepted for inclusion in Electronic Theses and Dissertations by an authorized administrator of Digital Commons @ East Tennessee State University. For more information, please contact digilib@etsu.edu.

Study of the Cell Membrane and the Synthesis of Chimeric Human Bacterial Phospholipids

---

A thesis

presented to

the faculty of the Department of Chemistry

East Tennessee State University

In partial fulfillment

of the requirements for the degree

Master of Science in Chemistry

---

by

Opeyemi Tade

December 2021

Dr. Robert Standaert, Chair

Dr. Aruna Kilaru

Dr. Ismael Kady

Keywords: phospholipids, cell membrane, laurdan, biofuel, general polarization (GP)

ABSTRACT

Study of Cell Membranes and the Synthesis of Chimeric Human Bacterial Phospholipids

by

Opeyemi Tade

Phospholipid bilayers are the principal component of the cell membrane. Membranes ensure the maintenance of processes required for cells' survival by regulating the inflow and outflow of nutrients and other molecules using membrane proteins. However, studying the cell membrane is challenging because of its complexity and small size. *In-vitro* membrane models made of phospholipids are important tools for studying membranes. In this work, we aim to study the fluidity of phospholipid bilayers of different lipids using general polarization (GP) of the fluorescent probe Laurdan as a measure. We will focus on the relative importance of head groups and fatty acids in the phospholipid. For this purpose, we are synthesizing chimeric lipids with the common human head group phosphocholine paired with bacterial fatty acids. We will compare the response of the human and chimeric lipids to temperature and biofuels to ascertain whether improved stress tolerance can be obtained with the chimeras.

ACKNOWLEDGMENTS

My sincere gratitude to God almighty for the grace to embark on this journey. I would like to sincerely appreciate my research advisor, Dr. Robert Standaert for his guidance, patience and mentorship throughout the program and an opportunity to be a part of his team.

I would like to appreciate Dr. Ismail Kady and Dr. Aruna Kilaru for accepting to be a part of my advisory committee and for their timely advice towards the progress of the research.

I would like to appreciate my colleagues: Enoch Asimbisa and John Hayford Teye-Kau, for their incomparable contributions and supports during the research. Special appreciation to East Tennessee State University (ETSU) for funding this research.

TABLE OF CONTENTS

LIST OF FIGURES

LIST OF ABBREVIATIONS

AcOH	Acetic acid
AcONa	Sodium acetate
BnBr	Benzyl bromide
BSTFA	*N*,*O-bis* (trimethylsilyl) trifluoroacetamide
m-CPBA	*meta*-Chloroperoxybenzoic acid
cps	Counts per second
DCC	*N*,*N*′-Dicyclohexylcarbodiimide
DCM	Dichloromethane
DMAP	4-Dimethylaminopyridine
DMSO	Dimethyl sulfoxide
EtOAC	Ethyl acetate
EtOH	Ethanol
FAME(s)	Fatty acid methyl ester(s)
FC	Flash chromatography
GC/MS	Gas chromatography/mass spectroscopy
GP	General polarization
GRAS	Generally recognized as safe
HMF	Hydroxymethylfurfural
Laurdan	6-Dodecanoyl-2-dimethylaminonaphthalene
LPC	Lysophosphatidylcholine
LUV	Large unilamellar vesicle
m/z	mass-to-charge ratio
MeOH	Methanol
MLV	Multilamellar vesicle
NEt_3	Triethylamine
NMR	Nuclear magnetic resonance
PA	Phosphatidic acid
PC	Phosphatidylcholine
POPC	1-Palmitoyl-2-oleoyl-*sn*-glycero-3-phosphocholine
PE	Phosphatidylethanolamine
PG	Phosphatidylglycerol
sn	Stereospecific numbering
TBAI	Tetra-*n*-butylammonium iodide
TFA	Trifluoroacetic acid
THF	Tetrahydrofuran
T_m	Phase transition temperature
TPS	2,4,6-triisopropylbenzenesulfonyl chloride

CHAPTER 1. INTRODUCTION

Understanding the function and structure of the cell membrane is one of the major challenges in life science, because of the small size and compositional complexity of the membrane. Embedded in a membrane are various components, including thousands of distinct lipids, proteins, and carbohydrates. All these components contribute to the function of the membrane including adaptation to various unfavorable environmental conditions. Of these, the lipids, particularly phospholipids, are the major building blocks.

The synthesis of artificially introduced enzymes by bacteria confers added abilities to transform organic molecules, which is essential in the production of important chemicals through fermentation, particularly biofuels. Microbes (bacteria and yeast) are an important source of industrial fine chemicals and biofuels; biofuels are used as supplements to the fuel supply to reduce total dependence on fossil fuel. However, exogenous molecules can be toxic to bacteria. In the case of biofuels, the desired products are toxic because they disrupt the cell membrane structure. Chemical solvents used in biofuel processing, such as tetrahydrofuran, also target the membrane. As a result, productivity and product yield become economically non-viable.[1]

Various research indicates the influence of phospholipid tail groups on bacterial adaptation to membrane disruptions caused by biofuels.[2–5] However, less is known of the influence of hydrophilic headgroups on membrane properties or adaptation to biofuels and organic solvents.[6] Hence, our research focuses on studying the influence of phospholipid headgroup on bacterial adaptation to biochemicals such as biofuels, and on head/tail combinations.

Biofuels

Biofuels are renewable fuels (such as alcohols, biodiesel, and biogas) obtained from biological sources, mainly plants. They are considered supplements and alternatives to nonrenewable fossil fuels used as transportation fuels. Fossil fuels are major source of global energy and are obtained from crude oil, coal and natural gas.[7,8] Unlike biofuels, fossil fuels are sourced from buried organic matter that has accumulated for millions of years and cannot be regenerated within a short period. As a result of increased industrialization and global population rate, the use of fossil fuel outmatches its regeneration and discovery rate, which results in increased demand for fossil fuel.[9] The increased demand results in fuel price hikes, total dependence on the limited crude oil-exporting countries, and scarcity that cannot be fully satisfied by the finite source of available fossil fuel.[10] Hence, continuous usage without supplements or alternatives might lead to the eventual exhaustion of fossil fuel sources. As a result, many countries including United States, Indonesia, Brazil, and Germany to mention a few, have implemented the use of biofuel/gasoline blends to reduce the consumption of fossil fuel and mitigate its side effects.[11]

In 1975, the production of biofuel took on prominence because of oil shortages. Microbial fermentation of sucrose and starch obtained from food crops such as sugarcane, corn, and beets promised to alleviate the situation. The biofuels synthesized were used as oxygenated additives and octane boosters in biofuel/gasoline blends to reduce total dependence on fossil fuels.[12] This method of biofuel synthesis from food crops is termed the first-generation biofuel. Although the process is simple, as it involves the fermentation of sucrose (a disaccharide) or starch (a soluble glucose polymer) by microorganisms, it is, however, unfavorable because food crops are diverted to biofuel production. The competition between the use of food crops for food

and biofuel production resulted in food shortages and increased food prices that threaten food security.[13] Efforts are in progress to mitigate these problems by expanding the choices of biomass sources from food crops to non-food lignocellulosic biomass. Biofuels from non-food biomass (lignocellulose) are termed second-generation biofuels. These include both ethanol and advanced fuel molecules like 1-butanol.

Lignocellulose as an Alternative Source of Biomass

Lignocellulose is the major supporting component of a plant cell and is made up of complex polymeric structures of lignin, hemicellulose and cellulose.

Cellulose is a linear homopolymer of D-glucose units connected by 1,4-β glycosidic linkages (Figure 1). Hemicellulose is a heterogeneous, branched heteropolymer that may contain xylose, arabinose, mannose, glucose and/or galactose. Lignin (Figure 2) is an extensively cross-linked phenolic polymer of phenylpropanoids (such as *p*-coumaryl alcohol, coniferyl alcohol and sinapyl alcohol) during biosynthesis, lignin is the major source of renewable phenolic compounds which are alternatives to phenolic compounds produced from fossil fuel.[14-16] The cellulose, lignin, and hemicellulose are intertwined into a complex structure of lignocellulose.

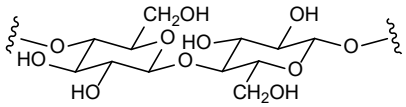

Figure 1. Structure of cellulose (poly-β-1,4-D-glucose)

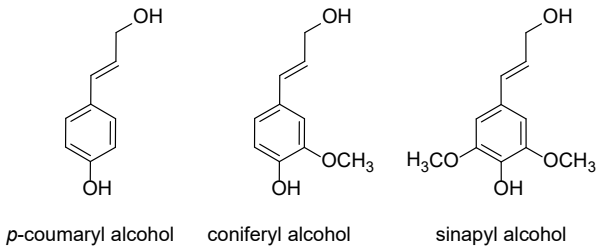

Figure 2. Phenylpropanoids involved in the biosynthesis of lignin

The refractory nature of lignocellulose promotes the survival of plants in their environment, including resistance to microbial attack. Examples of lignocellulosic feedstocks include herbaceous plants like switchgrass, woody trees like poplar, forest residues, residues from agriculture such as rice and wheat straws, and wood shavings, mostly generated as waste and currently discarded. Diverting such abundant material to biofuel and industrial chemical production is an effective way of reducing environmental pollution. Unlike food crops, lignocellulosic feedstocks are abundant and relatively cheap.[17]

Despite the beneficial attributes of lignocellulosic biomass, its structural complexity is a major setback to its application in biofuel synthesis. Unlike the first-generation biomass that provides readily fermentable sugars like sucrose (from sugarcane) or starch (corn, easily hydrolyzed to fermentable sugar), lignocellulosic biomass cannot be fermented directly (Figure 3). This refractoriness results from the insolubility and complexity of lignocellulose, which inhibits enzymatic degradation by microorganisms. As a result, thermochemical pretreatment is necessary to break down the structure, increase accessible surface area and expose the sugar components.[13] Pretreatment increases cost, consumes energy, and produces waste.

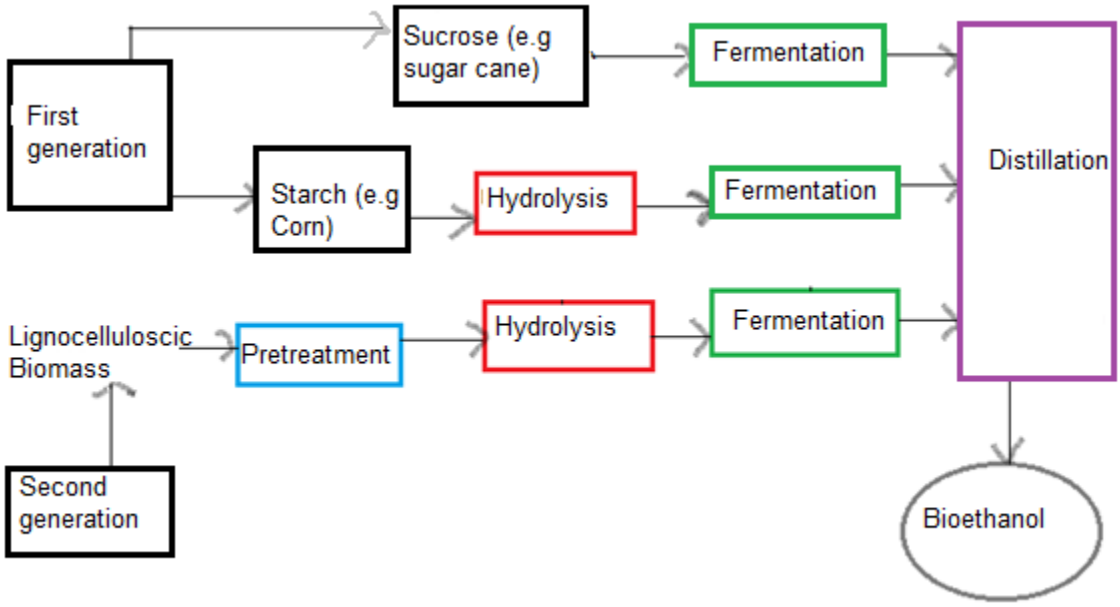

Figure 3. Flow chart showing the differences in the synthesis of first- and second-generation bioethanol

Biomass Pretreatment

The main current chemical pretreatment processes are acidic or alkaline hydrolysis, with dilute sulfuric acid being most common (0.1–1% sulfuric acid at 140–200 °C).[18] Organic cosolvents have also been found to be an effective pretreatment to enhance the production of biofuel and biochemicals. Currently employed solvents include formic acid, acetic acid and ethanol. More hydrophobic solvents can reduce precipitation of lignin in particular, the use of tetrahydrofuran (THF) as a cosolvent has been observed to effectively reduce the resistivity of lignocellulosic feedstock to give high yields of biofuel and other valuable non-fuel biochemicals such as levulinic acid, furfural, and HMF (5-hydroxymethyl furfural).[19,20] However, residual cosolvents and target products including the synthesized biofuels are toxic to microorganisms; biofuels are antimicrobials naturally.[21] Of most importance to the current work, they reduce cell viability by disrupting membrane fluidity, which interferes with the physiological processes of

the cell. The microorganism becomes weak or dies, and productivity falls such that economically viable levels of the product cannot be reached.[22] It is clear that to improve the production of biofuels and these important biochemicals, it is important to study the cell membrane to understand possible ways of improving bacteria's resistance to these solvent effects.

The Cell Membrane

The cell membrane is a dynamic, thin flexible layer that separates the cell's interior and exterior. It serves as a barrier and protective veil that compartmentalizes the internal components It is intrinsically impermeable to ions, polar molecules and macromolecules, so the membrane ensures a living cell remains stable in its environment. However, it has selective transport functions to regulate the inflow of essential nutrients, solutes, and gases, and the outflow of waste from the interior.[23]

The major components of the cell membrane are the phospholipids, which are arranged as a bilayer of apposing leaflets. Embedded in or associated with the bilayer are hundreds of proteins and some carbohydrates, all of which contribute to the diverse functions of the membrane.[23] Some of these functions include the transduction of energy and signals across the membrane, regulation of nutrient inflow, and adaptation of an organism in its environment. In addition to transport and signaling, the membranes also function as sites for other physiological or biochemical processes, such as identifying foreign bodies and recognizing cells, e.g., differentiating familiar cells from alien cells.

Recognition of cells (and their membrane) as the fundamental units of all living organisms emerged in the early 1830s. Unlike higher organisms, single-celled organisms like bacteria are exposed to harsh and unpredictable environmental conditions. To adapt to such varied environments, they have evolved sophisticated membranes to increase their chances of

survival. Despite the importance of the membrane to all life, there was a poor understanding of the membrane until the 1950s, especially with bacterial membranes because it was inconceivable to some that organisms thought to be simple could have a complex cell membrane.[24] It is now clear that the bacterial membrane has many similarities to the membranes of higher organisms.

In 1972, Singer and Nicholson proposed the fluid mosaic model for membrane structure.[25] They referred to the structure as mosaic because of the hundreds of important molecules embedded in and dispersed throughout the membrane, leading to a complex, heterogeneous structure. These components are free to diffuse laterally in the plane of the membrane to ensure optimum function of the cell, and thus the membrane can be viewed as a 2-dimensional fluid.[26] The two crucial components of the membranes are glycerophospholipids (phospholipids) and proteins.[27] Subsequent studies have shown that the fluid mosaic model is somewhat oversimplified and that there is a lateral organization within the membrane. That is, more ordered clusters of lipids and proteins, termed membrane domains or lipid rafts, segregate from the bulk phase.[28] Membrane domains are thought to be important in signal transduction generally to help regulate the death and growth of the cell. Bacterial membranes are also believed to have membrane domains, another important parallel with the membranes of higher organisms.[29,30]

Hence, the survival of every living organism is dependent on the cell membrane. As a result, studying the cell membrane has been an important field relevant to many disciplines. In biomedicine, it gives information on the interaction of cells with their environment and how they respond to threats, to understand and combat diseases.[31] In bioremediation and biofuel synthesis, studying the cell membrane proffers an understanding of toxic effects on microbial membranes

and possible ways of engineering microorganisms to enhance their biosynthetic or degradative properties.

The disruption of the cell membrane by biofuels (and biochemicals) and residual cosolvents used in biomass treatment is a major challenge. Damage occurs by the accumulation of the solvents in the lipid bilayer. They increase the entropy of the bilayer, resulting in thinning and fluidization of the membrane, as well as the denaturation of membrane proteins, a process known as chaotropicity.[21] Since the lipid bilayer is made up of phospholipids, it is important to understand phospholipids and their components.

Phospholipids

Phospholipids are the major component of the cell membrane. They are amphipathic molecules with polar, hydrophilic head groups and non-polar hydrophobic tail groups. They self-assemble into the bilayer structure of cell membranes and are arranged as leaflets with the hydrophobic groups shielded from the aqueous surface while the hydrophilic groups are exposed to the exterior (aqueous surfaces). To ensure that the hydrophobic tail groups are not exposed to the aqueous environment, the phospholipid bilayer forms closed spherical structures called vesicles. These arrangements of the phospholipids are responsible for the architecture of the cell membrane.[32,33]

Phospholipids are formed from a pair of hydrophobic fatty acids and a polar phosphate moiety attached to a glycerol backbone**.** The phosphate moiety may be a simple phosphate but is more commonly esterified to one of several common alcohols, (choline, ethanolamine or glycerol), hence the headgroups are named as phosphocholine, phosphoethanolamine and phosphoglycerol, (Figure 4).[32,33] The complete lipids (with glycerol and fatty acids attached to

the head group) are described as phosphatidylcholine (PC), phosphatidylethanolamine (PE) or phosphatidylglycerol (PG), respectively.

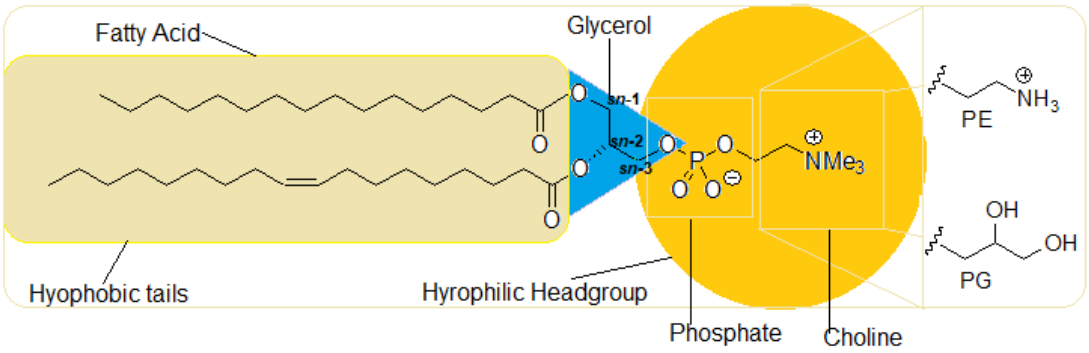

Figure 4. Structure of phospholipids with common head groups. Phosphocholine (PC), Phosphoethanolamine (PE) and Phosphoglycerol (PG). A large number of different fatty acids is encountered in nature

PC and PE phospholipids are the most common phospholipids found in human and bacterial cell membranes, respectively (Figure 6 A and B). Most bacteria contain 75% PE and 15–20% PG. Only a few species contain PC in their membrane structures (e.g., *Rhodopseudomonas sphaeroides and Pseudomonas stutzeri*).[34]

The phospholipids are named using stereospecific numbering (*sn*), such that the phosphate head group is attached at position *sn*-3 to create the (*R*) configuration at *sn*-2. Fatty acids are esterified to the *sn*-1 and *sn*-2 hydroxyls of glycerol. Depending on the organism or species, unsaturated chains or branched-chain fatty acids mostly are found at *sn*-2, whereas the saturated fatty acids are found more commonly at *sn*-1. Phospholipids containing only one fatty acid are called lysophospholipids, e.g., lyso-phosphatidylcholine (Figure 5D, LPC).[34] A wide variety of fatty acids differing in chain length (~C_{12} to C_{22}, with C_{14}–C_{18} being most common), number and location of double bonds (unsaturation), branching pattern, and chain modifications

(cyclopropanation and hydroxylation, for example) are encountered in natural systems. Relevant examples will be discussed in context below.

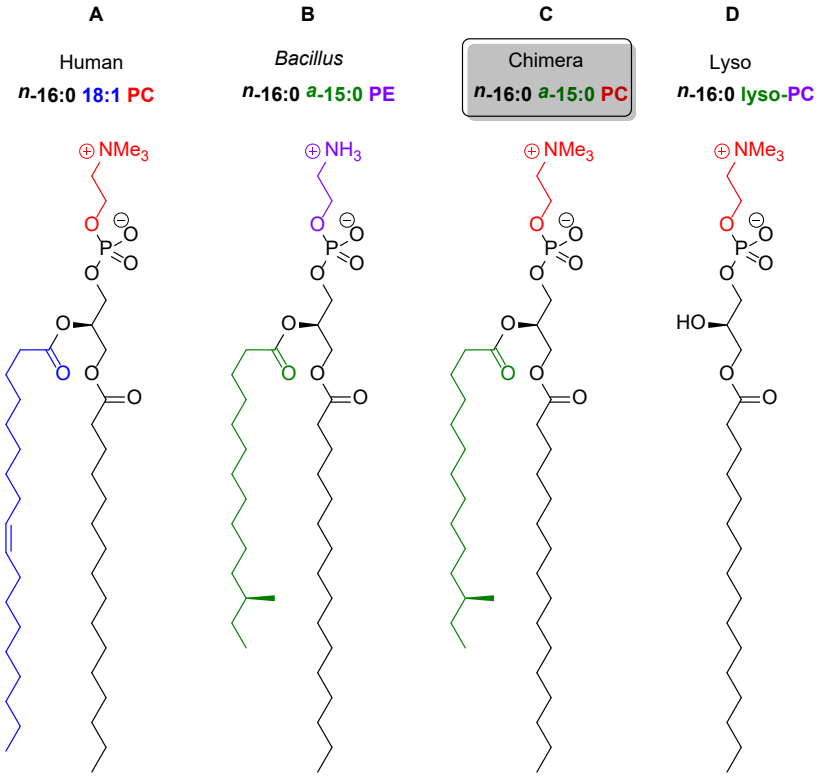

Figure 5. Structures of representative phospholipids from humans and bacteria (*Bacillus subtilis*), along with a proposed chimera. (A) phosphatidylcholine (PC), (B) phosphatidylethanolamine (PE), (C) human–bacterial chimeric phospholipid and (D) lysophosphatidylcholine (LPC)

Membrane Fluidity

Membrane fluidity is a bulk property reflecting the degree of molecular motion and disorder within the lipid bilayer. It is an important property of the membrane and needs to be maintained at the proper level (irrespective of environmental stress) to preserve the structure and function of the membrane components, including membrane proteins. A slight change in membrane fluidity can greatly perturb the normal cell function.[35,36]

The lipid bilayer undergoes a reversible phase change between fluid (disordered) and non-fluid (gel) states. The temperature at which this change occurs is known as the phase transition temperature (T_m). This order–disorder phase transition is greatly affected by the phospholipid composition,[37-39] in particular the fatty acid composition in terms of chain length, branching and unsaturation. Straight, saturated chains pack more tightly hence reduce fluidity. The *cis* double bond forms a kink in the chain and inhibits the tight packing of the fatty acid chains, increasing fluidity. A common example in eukaryotes is oleic acid. This fatty acid is shown in Figure 5A at the *sn*-2 position of 16:0 18:1 PC, commonly known as POPC (1-palmitoyl 2-oleoyl PC). As will be discussed below, bacteria of the type relevant to our studies more commonly employ branched fatty acid to inhibit packing and fluidize the membrane. An example is anteisopentadecanoic acid (12-methyltetradecanoic acid, a-15:0), as shown at the *sn*-2 position in Figures 5B and 5C. In all cases, longer chains decrease fluidity.

Research has demonstrated that alterations to fatty acid composition are an important adaptation to environmental stress. In an early investigation, Marr and Ingram studied *Escherichia coli* and found a decrease in the proportion of cis-11-octadecenoic acid (vaccenic acid, the most abundant unsaturated fatty acid in *E. coli*) and an increase in the proportion of palmitic acid (the most abundant saturated fatty acid) with increasing temperature.[40]

Disruption of the microbial cell membrane and alteration of membrane fluidity are of major concern in biofuel synthesis because fuel and solvent molecules accumulate in the membrane, generally increasing fluidity and permeability of the membrane. One adverse consequence is ion leakage, which results in loss of membrane potential and decreased cell growth as the bacteria struggle to survive rather than produce more biofuel.[41,42] Heipieper and de Bont investigated the adaptation of *Pseudomonas putida* to ethanol and elevated temperature,

both of which fluidize membranes.[43] Cerulenin, an inhibitor of fatty acid biosynthesis, was introduced to prevent the bacteria from adaptation by the synthesis of longer fatty acids. In response, the bacteria produced *trans*-fatty acids from existing *cis*-fatty acids using a *cis–trans* isomerase. *Trans*-unsaturated chains pack almost as tightly as saturated chains, and the isomerization allowed an urgent response to the unfavorable conditions by decreasing fluidity.

Vollherbst-Schneck et al. studied *Clostridium acetobutylicum* showed inhibition of glucose absorption, growth and active transport of nutrients in response to 1-butanol. After the synthesis of 1-butanol to about 0.2% by the bacteria, an increase in saturated fatty acids and a decrease in unsaturated fatty acids was observed.[44,45] Wilbanks and Trinh studied the toxic effects of eight alcohols (ethanol, propanol, isopropanol, 1-butanol, isobutanol, 1-pentanol, isopentanol and 1-hexanol) on the growth of *E. coli*. They observed increased growth inhibition as the concentration and chain length of alcohol increased. Reductions in growth rates were 18% at 15 g/L with ethanol, 50% at 7.5 g/L with 1-butanol, and 45% at 0.695 g/L with 1-hexanol. No growth at all was observed with 1-hexanol at 2.5 g/L.[46]

As discussed above, the adverse effects of biofuels on cell membranes can reduce the efficiency of bacteria in biofuel production. One of the methods used to improve biofuel productivity is genetic manipulation of bacteria, and the susceptibility of the membrane to solvents and fuels suggests it as an opportune target. However, a rational basis for modifying the membrane composition does not yet exist, and engineering native biofuel-producing bacteria is challenging.[47] These limitations argue for the use of tractable model organisms and *in-vitro* membrane models. In this research, the focus is on membrane models of the bacterium *Bacillus subtilis.*

Assessment of Membrane Fluidity

The most common method for investigating membrane fluidity relies on the use of fluorescence probes. Laurdan (Figure 6) is the most widely used probe because it is environmentally sensitive and changes fluorescence properties based on differences in polarity,[48] making it sensitive to phase transitions, changes in membrane fluidity and water penetration.[49]

Laurdan has a push-pull arrangement of an electron donating dimethylamino group an electron-accepting carbonyl group conjugated through the 2- and 6- positions, respectively, of naphthalene. The rigid bicyclic nucleus is important, as the maximum fluorescence effects are observed when these groups are at a maximum distance (Figure 6) to create the largest dipole moment.[50]

Laurdan partitions into the bilayer with its fatty acid chains (lauroyl) embedded in the lipid bilayer, while its naphthalene moiety is in the head group region, the order and water penetration of which vary with lipid packing and fluidity.[51] When Laurdan is excited by light, its dipole moment increases dramatically, and polar solvents in the vicinity will rearrange to optimize dipole-dipole interactions, stabilizing the excited state. The result is a red-shift in the emission spectrum of the probe in polar environments.[52]

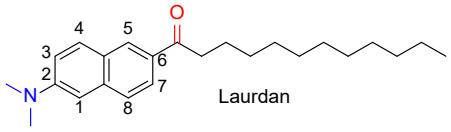

Figure 6. Structure of Laurdan (6-dodecanoyl-*N*,*N*-dimethyl-2-naphthylamine).

In a tightly-packed gel-phase bilayer, Laurdan is shielded from the highly polar, mobile water molecules and gives maximum emission at 440 nm (blue shift). In a highly disordered fluid phase, Laurdan is exposed to water and gives a maximum emission at 490 nm (red shift).[52] In fluid phases of intermediate order, maxima at both 440 and 490 nm are observed. The relative

contributions of red- and blue-shifts reflect fluidity and are quantified by calculating the general emission polarization value (GP), given by Equation 1.1.

$$GP = \frac{I_B - I_R}{I_B + I_R} \quad (1.1)$$

where I_B and I_R represent emission intensities at 440 and 490 nm, respectively. A decrease in GP value indicates a transition from a more ordered bilayer to a more fluid (disordered) bilayer with greater water penetration.[52,53] For this work, the fluidity of cell membrane distorted by biofuels and cosolvent treatment will be assessed by determining the general polarization of Laurdan.

Bacillus subtilis and its Important Fatty Acids

B. subtilis is an aerobic, single-celled Gram-positive bacterium as classified by Christian Gram's staining procedure. It is easy to grow, nonpathogenic and generally recognized as safe (GRAS). It has a well-characterized membrane composition and excellent genetic tools available for engineering. It is also the first Gram-positive bacterium to be sequenced genetically[23,54] It has been a model microorganism for understanding spore-forming Gram-positive bacteria and pathogenic *Bacillus* species. Due to these outstanding characteristics, it is an important organism in biotechnology and is referred to as a cell factory for the synthesis of extensive products ranging from proteins to biochemicals.[55,56] However, its membrane lipids are not commercially available, so *in-vitro* studies have lagged.[57]

B.subtilis contains predominantly saturated fatty acids. While some of these have straight (unbranched or normal) chains, such as hexadecanoic acid (palmitic acid), most bear methyl branches at the penultimate or antepenultimate carbons (iso- and anteiso- fatty acids, respectively, Figure 7). Fatty acids are given abbreviated names based on number of carbons, number of unsaturations and branching patterns. For example, palmitic acid is 16:0, isopalmitic acid (14-methylpentadecanoic acid) is i-16:0 and anteisopalmitic acid (13-methylpentadecanoic

acid) is a-16:0. The six most common branched-chain fatty acids in *B. subtillus* are shown in Figure 9. These branched-chain fatty acids predominate in Gram-positive bacteria but are only minor constituents in Gram-negative bacteria like *Escherichia coli* and *Streptococci*.[58,59] The six most common branched fatty acids and one less common unsaturated fatty acid are depicted in Figure 7.[60,61]

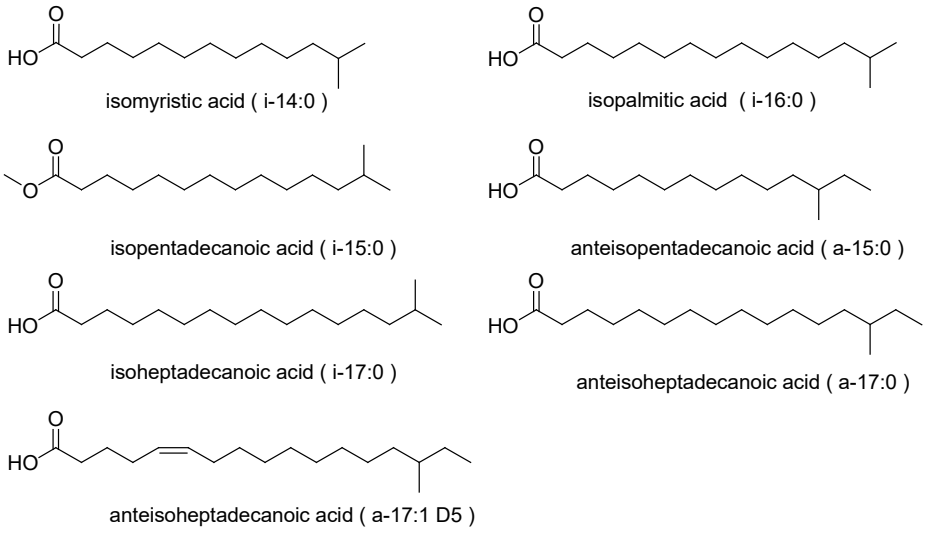

Figure 7. Fatty acids of the *Bacillus subtilis* membrane

Anteiso-branched-chain fatty acids have a lower melting point relative to iso-branched-chain fatty acids, but branches are not as effective as cis double bonds in lowering the temperature of the gel-to-liquid phase transition in the membrane. Unsaturated fatty acids are normally minor components of the *B. subtilis* membrane, whereas they are major components of the membranes in Gram-negative bacteria and higher organisms. *B. subtilis* does have the capacity to desaturate fatty acids and uses it in rapid adaptation to cold shock, for example by converting a-17:0 to a-17:1 (Δ^5) (Figure 7). In long-term adaptation, *B. subtilis* decreases the amount of iso-branched fatty acids and increases the amount of lower-melting anteiso-branched fatty acids.[62,63]

Lipid Vesicles

In general, studying bacterial cell membranes is a challenging task. As a result of the structural complexity of natural membranes, lipid vesicles (liposomes) constructed from chemically defined phospholipids are often employed as membrane models. Vesicles provide a stripped-down model of the membrane with only a lipid bilayer of well-defined composition. Use of model membranes simplifies the system and allows the use of a wide range of chemical and biophysical techniques to be employed.[64]

Vesicles form spontaneously when many common phospholipids are dispersed in an aqueous medium. PC and PG lipids are in this category. Depending on lipid structure and geometry, particularly the size and shape of the head and tail groups, other supramolecular arrangements are possible. Phospholipids with similar sizes for head and tail groups as in PC and PG (Figure 8) have pseudo-cylindrical structures and form stable lipid bilayers. Lipids with one tail, such as lysophosphatidylcholine (LPC), have a conical structure, with a larger diameter at the head, giving them an intrinsic curvature that leads to the formation of micelles rather than bilayers (Figure 9). At the other extreme, lipids with relatively larger tails than heads, as in PE (Figure 10), have negative intrinsic curvature and form an inverted hexagonal phase.[65] When mixed with PC or PG lipids, PE can be incorporated into a lipid bilayer.

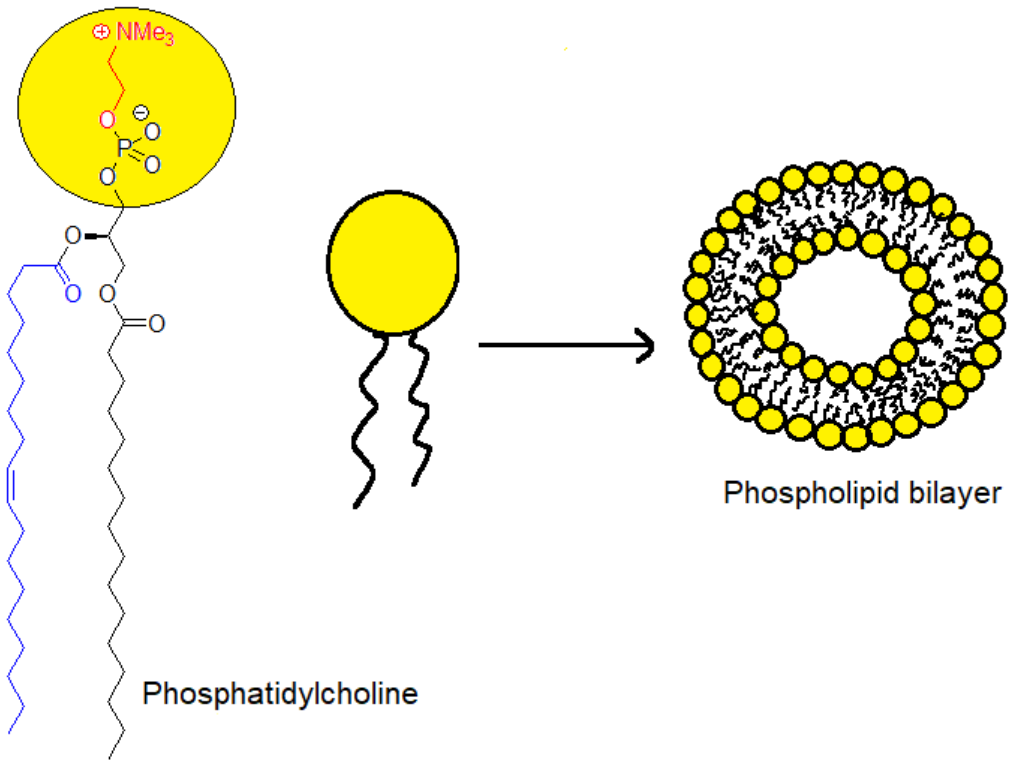

Figure 8. Formation of a lipid bilayer by phosphatidylcholine (PC). PC lipids have matched diameters in heads and tails, giving them a cylindrical cross-section that packs into planar lipid bilayers

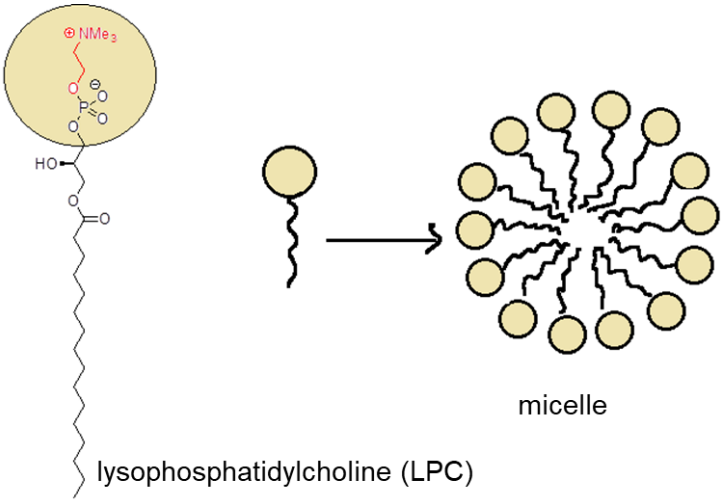

Figure 9. Formation of micelles by lysophosphatidylcholine (LPC). LPC has a smaller tail group and larger headgroup, giving it an inverted conical shape that assembles into micelles (spheroidal monolayers with heads exposed to water)

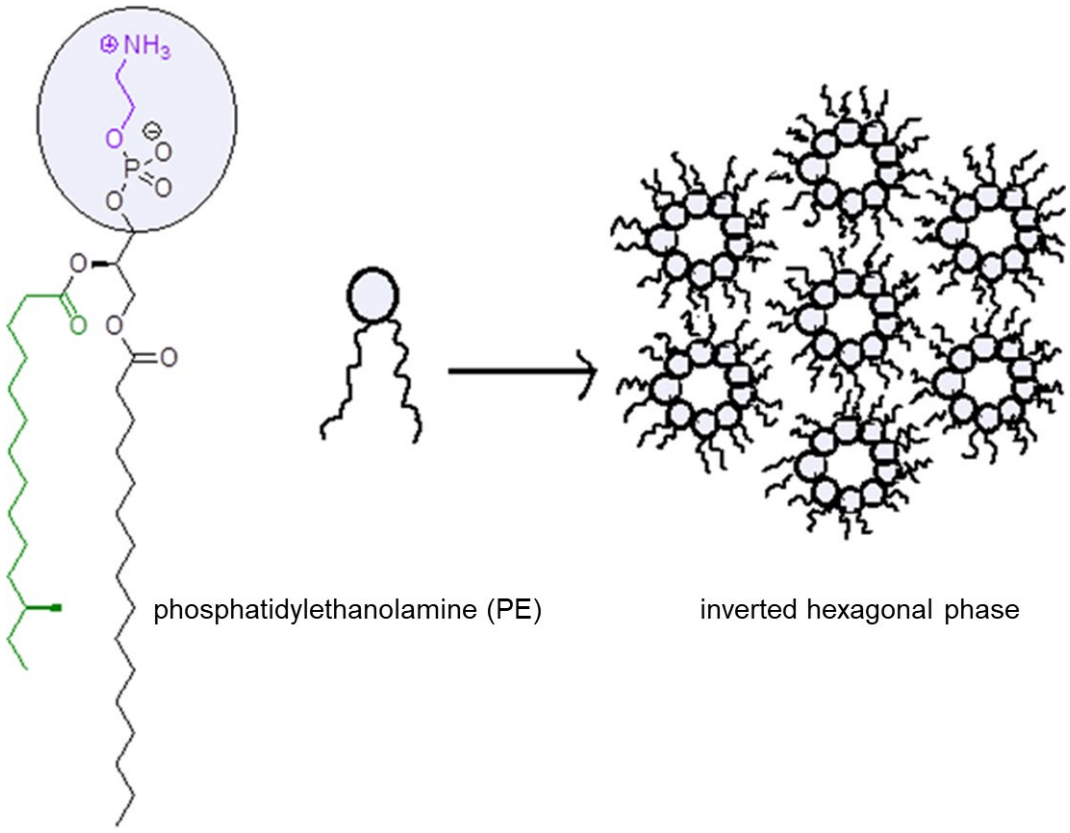

Figure 10. Formation of the inverted hexagonal phase by phosphatidylethanolamine (PE). The relatively small head group in PE gives it a conical shape and precludes formation of stable bilayers

Vesicles have a number of applications outside membrane research. Their small size, amphipathic nature, low permeability and biocompatibility has made them common platforms in drug delivery. They can be used to packaging either hydrophilic or hydrophobic drugs, they can be used to control drug release, and they can reduce drug toxicity (Figure 11).[66]

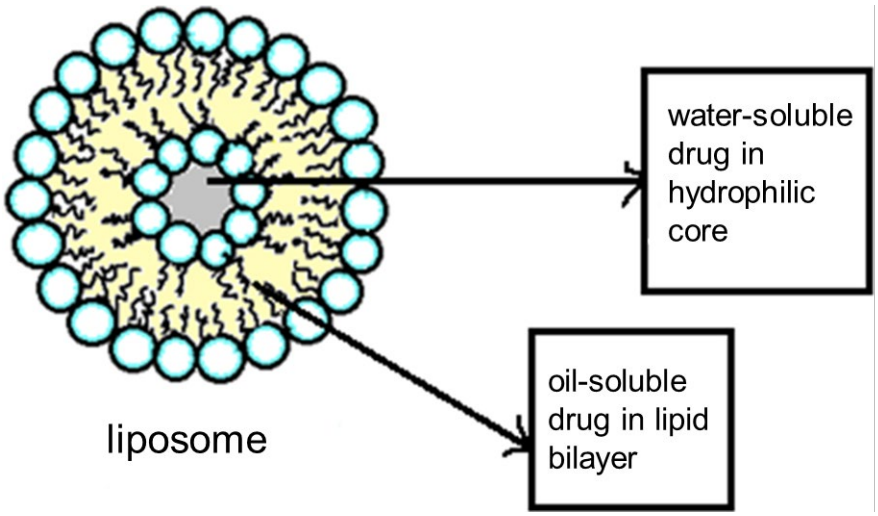

Figure 11. Liposomes (unilamellar vesicles) used to package drugs

Vesicles can be either unilamellar (a single bilayer, like a cell membrane) or multilamellar (having multiple, concentrically stacked bilayers in an onion-like structure).[67] PC lipids are zwitterionic and electrically neutral, which promotes the formation of multilamellar vesicles (MLVs) upon hydration of the phospholipids. These vesicles can then be converted to uniformly sized large unilamellar vesicles (LUVs) 50–500 nm in diameter by extrusion through a nanoporous membrane with the corresponding pore size. Small unilamellar vesicles (SUVs, < 50 nm in diameter) are produced by sonication.[68]

The source of phospholipids is critical for making vesicles suited for a particular lipid. Either synthetic or natural phospholipids can be employed. Natural phospholipids (e.g., from egg yolk or soybeans) are relatively inexpensive, but they are complex mixtures, and price increases with increasing purity. Synthetic phospholipids are expensive but are usually of higher purity and allow for the creation of defined lipid mixtures such that the effects of specific head/tail combinations and compositions can be studied. The present work requires chimeric phospholipids that are necessarily synthetic and are not commercially available.[66] These

considerations motivate the total synthesis of novel phospholipids for the study of fuel/solvent tolerance in model systems. The complete flexibility of tailoring the fatty acid chains and headgroup moieties provides a great advantage.

Synthesis of Phospholipids

Several synthetic routes have been reported for the synthesis of phospholipids, but only a few have effectively synthesized phospholipids with different fatty acid chains. The synthesis of diacylglycerols from D-mannitol reported by Virtanen et.al involves the tritylation of D-mannitol (**1)** to give 1,6-ditrityl- D-mannitol (**2**), was followed by oxidative cleavage and reduction to 1-trityl-*sn*-glycerol (**3**), subsequent acylation to 1-trityl-2,3-diacyl-*sn*-glycerol (**4**) and detritylation to form the phospholipid (**5**).[69] This synthetic route can be used only to synthesize symmetrically diacylated glycerols, and other methods must be employed to install a head group (Figure 12).

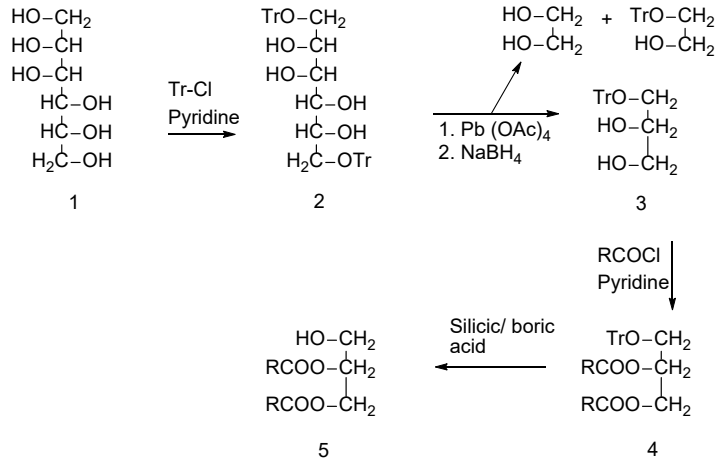

Figure 12. Synthesis of diacylglycerol from D-mannitol[69]

Another method that allows the installation of different fatty acids into PG lipids was reported by Gagnon et al.[70] This synthetic route involves the reaction between phenyl

dichlorophosphate (**6**), solketal (**7**), and (*S*)-glycidol (**8**) to give the phosphotriester intermediate (**9**) with a reported yield of 29%. This reaction was carried out in the presence of 2,2,6,6-tetramethylpiperidine as a base. Optimization of the reaction to increase the yield of phosphotriester to 94% was done by the addition of solketal before (*S*)-glycidol and the replacement of 2,2,6,6-tetramethylpiperidine with triethylamine. The epoxide ring-opening with myristic and palmitic fatty acid tail groups gave the protected intermediate (**10**). Deprotection was done by subsequent removal of the benzyl group by catalytic hydrogenation and acetonide deprotection in acidic condition (acetic acid) to produce the phosphatidylglycerol (**11**) (Figure 13). However, this route leads to the formation of side products that create difficult purification problems, the addition of the second acyl chain is difficult and causes the deprotection of the phenyl group and protecting group replacement by benzylation can lead to the migration of the phosphate group.

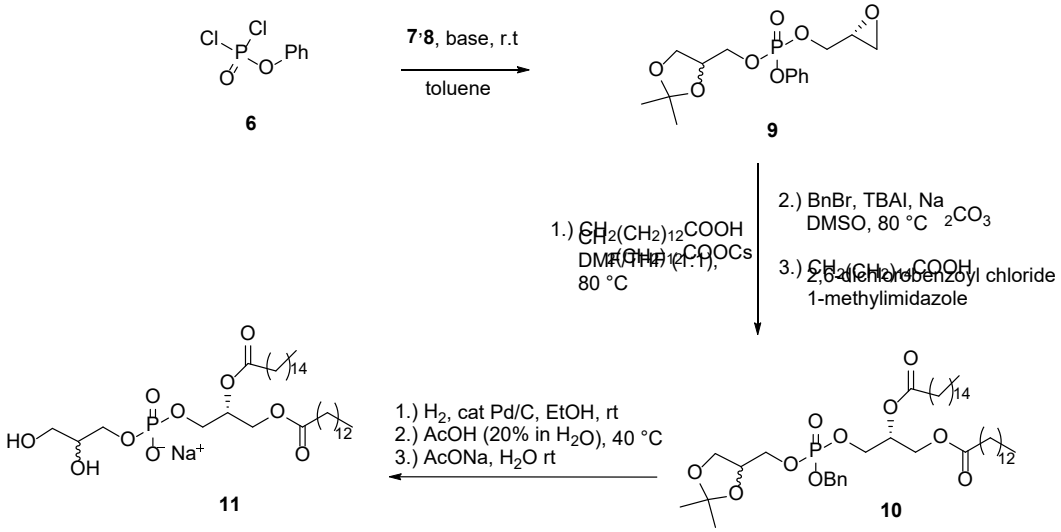

Figure 13. Synthesis of phosphatidylglycerol. BnBr, TBAI, DMSO, AcOH, AcONa and EtOH represent benzyl bromide, tetrabutylammonium iodide, dimethyl sulfoxide, acetic acid, sodium acetate and ethanol, respectively[70]

An efficient and versatile route toward several phospholipid types was published by Lindberg et al.[71] The key step involves the phosphorylation of (*S*)-glycidol (**12**) by a phosphoramidite (**13**), producing a phosphite ester (**14**) that is oxidized *in situ* with *meta*-chloroperoxylbenzoic acid (*m*-CPBA) to an *O*-protected phosphonoglycidol, phosphate ester (**15**). The *sn*-1 acyl chain is introduced by nucleophilic opening of the epoxide ring using the cesium salt of the required fatty acid. The *sn*-2 acyl group is introduced in the conventional manner using DCC and DMAP. Subsequently, the phosphate group can be deprotected and elaborated into PC, PG or PE lipids using appropriate methods. The route allows the flexibility of attaching different acyl groups to the glycerol backbone and the production of various phospholipids from phosphatidic acid (**16**) without tedious group protections and excessive side product formation. The overall route proposed is shown in Figure 14.

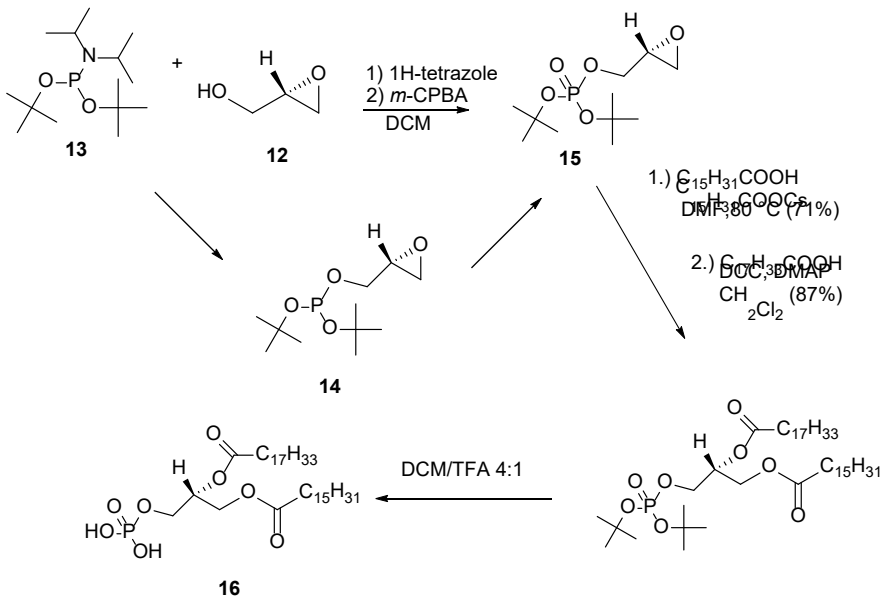

Figure 14. Reaction scheme for the synthesis of phospholipids. *m*-CPBA, DCM, DCC, DMAP and TFA represent *meta*-chloroperoxybenzoic acid, dichloromethane, dicyclohexycarbodiimide, 4-(dimethylamino)pyridine and trifluoroacetic acid, respectively [71]

After synthesis, the phospholipids derived by installing a head group on **16** will be incorporated into the desired vesicles by extrusion. Vesicles will be used as membrane models to assess membrane order and fluidity under the influence of temperature, alcohols, and organic solvent such as THF. All of these are stressors a bacterial cell is subjected to during the synthesis of biochemicals. Their effects can be gauged through their impact on membrane fluidity through general polarization of Laurdan fluorescence.

Research Objectives

The objectives of this research are:

- To synthesize the distinctive fatty acids prevalent in the *B. subtilis* cell membrane.
- To synthesize chimeric phospholipids containing the PC headgroup prevalent in the human cell membrane and tail groups prevalent in the *B. subtilis* membrane.
- To construct model membranes from commercially available (POPC) and synthesized phospholipids. These models make it possible to ascertain whether improved stress tolerance can be obtained with the chimeras (Figure 7).
- To study and compare the fluidity of the phospholipid bilayers in response to stress from temperature and biofuels/solvents (ethanol, 1-butanol and THF) using Laurdan as a fluorescence probe.
- To ascertain the relative role of head groups and fatty-acid chains of phospholipids on sensitivity or resistance to biofuels and solvents and temperature.

CHAPTER 2. EXPERIMENTAL METHODS

Reagents and Chemicals

Anhydrous tetrahydrofuran (THF), 1*H*-tetrazole, and triethylamine (NEt_3) were purchased from Alfa Aesar. Lithium tetrachlorocuprate (Li_2CuCl_4), methanol, hydrochloric acid, hexane, dichloromethane (DCM, CH_2Cl_2), toluene, anhydrous sodium sulfate (Na_2SO_4), hydrobromic acid (47-49%), ethyl acetate (EtOAc), and anhydrous ether were purchased from Fischer Scientific. 11-Bromoundecanoic acid, 12-hydroxydodecanoic acid, isopentylmagnesium bromide (2.0 M in diethyl ether), 2-methylbutylmagnesium chloride (2.0 M in diethyl ether), *sec*-butylmagnesium chloride (1.2 M in THF), isobutylmagnesium chloride (2.0 M in THF) and isopropylmagnesium chloride (2.0 M in THF) were purchased from Sigma Aldrich. 1-Palmitoyl-2-oleoyl-*sn*-glycero-3-phosphocholine (POPC), the vesicle extruder, Nucleopore track-etch membranes (19 mm diameter, 0.1 μm pore size), and filter supports (10 mm diameter) were purchased from Avanti Polar Lipids. (*S*)-Glycidol was purchased from TCI America. Sulfuric acid (H_2SO_4), sodium sulfide (Na_2S), dimethyl sulfoxide (DMSO), chloroform, ethanol, di-*tert*-butyl-*N*,*N*-diisopropylphosphoramidite, *meta*-chloroperoxybenzoic (*m*-CPBA), chloroform-*d*, and *N*,*N*-bis(trimethylsilyl)trifluoroacetamide (BSTFA) containing 1% chlorotrimethylsilane were obtained from Acros Organics. Anhydrous sodium thiosulfate ($Na_2S_2O_3$) and sodium bicarbonate were purchased from J.T Baker.

Instrumental Characterization of Samples

NMR Spectroscopy

Proton (^1H) and carbon (^{13}C) NMR (Nuclear Magnetic Resonance) analyses were carried out on a JEOL Eclipse 400 spectrometer. Chemical shifts were referenced to solvent (δ_H = 7.25

and δ_C = 76.8 for $CDCl_3$). Multiplicities are denoted as s, d, t, q, p, or m to represent singlet, doublet, triplet, quartet, pentet, or multiplet, respectively.

GC/MS Analysis

GC/MS (Gas chromatography/mass spectroscopy) analysis was performed using Shimadzu GC-2010 instrument equipped with an AOC-20i autosampler, an SHRXI-5MS capillary column (length 30 m, inside diameter 0.25 mm, film thickness 0.25 μm) and a GCMS-QP2010 mass-sensitive detector operating in electron impact mode at 70eV.

Analyses were performed using He carrier gas at a flow rate of 1 mL/min, an inlet temperature of 260 ℃, an ion-source temperature of 200 ℃, and a transfer line temperature of 250 ℃. The initial oven temperature of 50 ℃ was held for 2 min, ramped at 20 ℃/min to 280 ℃, and held for 2 min. An injection volume of 1 μL and a split ratio of 20:1 were used.

Fatty acid synthesis was monitored by GC/MS to ensure complete reaction and ascertain the purity and identity of the acids. The fatty acid samples were analyzed as their derived methyl esters (FAMEs). Methylation was performed by placing a small sample of material (0.5 μL of reaction mixtures, ~0.1 mg of solid samples) in a 13 × 100 mm screw-cap test tube, adding 1 mL of 10% conc. HCl in methanol, mixing, sealing the tube, and heating for 2 h at 80 ℃. After the solution had cooled to room temperature, hexane (1 mL) and deionized water (1 mL) were added. The sample was vortex-mixed for 10 s, and after the layers had separated, the top (hexane) layer was transferred to a 2-mL autosampler vial for GC/MS analysis.

Derivatization of 12-bromododecanoic acid was performed by trimethylsilylation rather than methylation because partial substitution of chlorine for bromine was observed after methylation. A 2-mg portion of the sample was placed into a test tube, and 1 mL of hexane was added. A 10 μL aliquot of the solution (~20 μg of sample) was transferred into a 2-mL

autosampler vial, 100 μL of BSTFA was added, and the vial was capped. After 1 h, the solution was diluted with 900 μL of hexane and analysed by GC/MS.

Spectrofluorimetric Analysis

Fluorescence emission spectra of Laurdan in the prepared vesicles were obtained using an excitation wavelength of 350 nm, with excitation and emission slits at 0.25 nm and 2.00 nm respectively. General polarization (GP) of Laurdan was calculated as $GP = (I_{440} - I_{490})/(I_{440} + I_{490})$ (Eq. 1.1)

Experimental Procedures

Preparation of Laurdan-Doped Unilamellar Vesicles

POPC vesicles containing 0.5 mol % Laurdan were prepared as follows. A stock solution of Laurdan (93 μM) in methanol (0.35 mL, 32.9 nmol) was mixed with 0.50 mL (5.0 mg, 6.58 mmol) of POPC (10 mg/mL in chloroform) in an amber glass dram vial. The solvent was evaporated under a stream of nitrogen, and residual solvent was removed by re-dissolving the lipids in chloroform, re-evaporating under nitrogen, and placing the mixture in a vacuum oven for about 12 h (overnight) to form a dry lipid film.

The lipid film was hydrated by adding 1 mL of deionized water, affording a cloudy suspension of multilamellar vesicles. Five sequential freeze-thaw cycles were performed using a dry ice–ethanol bath for freezing and a water bath at 50 ℃ for thawing, with intermittent vortex mixing over a 2 min period during the thaw phase. During this process, the suspension becomes less cloudy. The hydrated lipid suspension was then extruded 31 times at 40 ℃ using the Avanti mini extruder according to the manufacturer's instructions. Emission spectra of Laurdan were taken at 20 ℃, 29.5 ℃, 37.7 ℃ and 48.8 ℃ to assess changes in membrane fluidity.

Synthesis of Fatty Acids

The essential starting materials for the synthesis of fatty acids are 11-bromododecanoic acid, 12-bromododecanoic acid, Grignard reagents, THF (as solvent) and Li_2CuCl_4 as the coupling catalyst. All reagents were commercially obtained with the exception of 12-bromododecanoic acid, which was synthesized from commercial 12-hydroxydodecanoic acid for use in the synthesis of *a*-17:0 and *i*-17:0.

Synthesis of 12-Bromododecanoic Acid

The procedure used was from Makita et al.[72] and Lewis et al.[73] (Figure 15). To a round bottom flask containing a stir bar was added 4.0 g of 12-hydroxydodecanoic acid and 4.0 mL of 47% hydrobromic acid. The mixture was refluxed for 4 h, after which an extra 4 mL of 47% hydrobromic acid was added, and reflux was resumed for another 4 h. After cooling to room temperature, the reaction mixture was diluted with deionized water and extracted three times using DCM. The combined organic layers were dried over anhydrous Na_2SO_4, and the solvent was removed by a rotary evaporation to afford 4.37 g (85%) of the product as a yellow solid (Figure 16 A). This crude product was recrystallized from hexane to obtain a 3.49 g (80%) of the product as a white powder (Figure 16 B). The product was analyzed by GC/MS after derivatization by trimethylsilylation using BSTFA (Figure 17). ^{1}H NMR (400 MHz, $CDCl_3$) δ (ppm) 1.25 (s, 12H), 1.40 (p, 2H, *J*= 7.0 Hz), 1.61 (p, 2H, *J* = 7.3 Hz), 1.83 (p, 2H *J*= 7.2 Hz), 2.33 (t, 2H, *J* = 7.6 Hz), 3.39 (t, 2H, *J* = 7.0 Hz), 10.56 (br, 1H). The ^{1}H NMR data matched those reported in the Aldrich NMR Library.

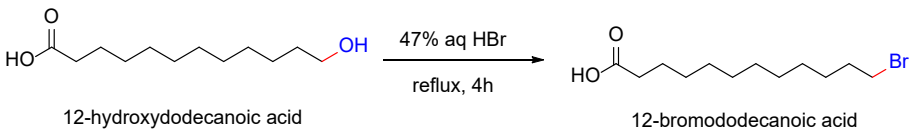

Figure 15. Synthesis of 12-bromododecanoic acid from 12-hydroxydodecanoic acid and hydrobromic acid

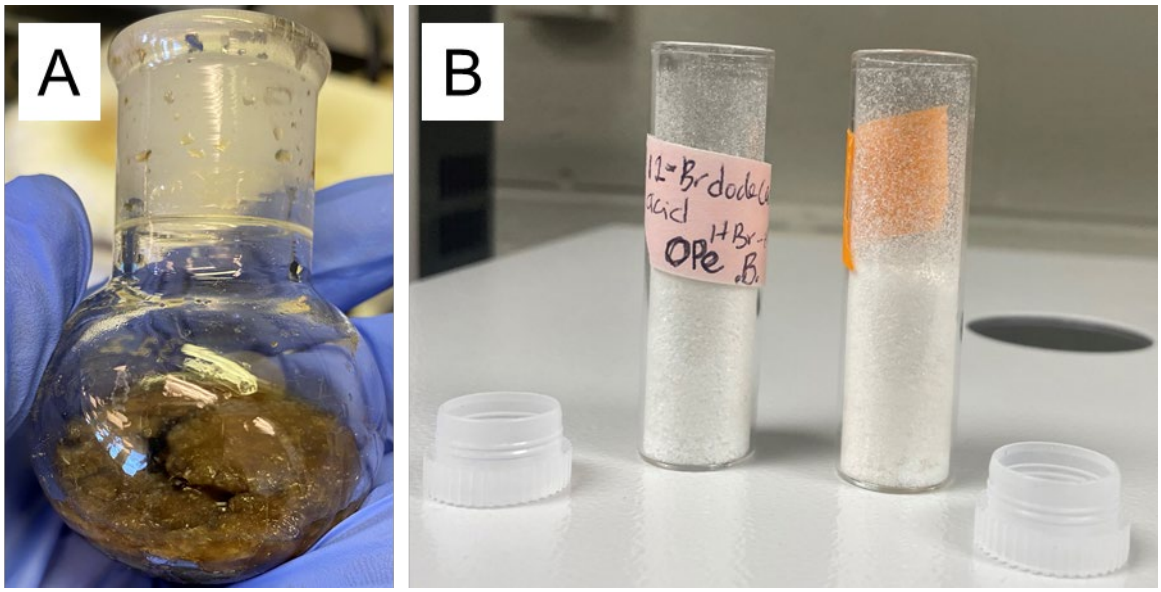

Figure 16. Crude (A) and recrystallized (B) 12-bromododecanoic acid

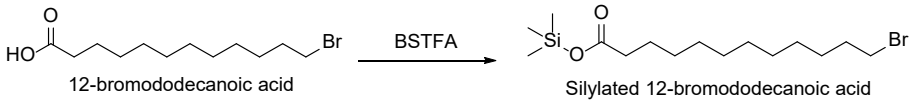

Figure 17. Derivatization by trimethylsilylation using BSTFA

Synthesis of Fatty Acids from 11-Bromododecanoic Acid

The fatty acids were synthesized as described by Baer and Carney[74] with slight modifications; extraction into potassium hydroxide was not carried out to prevent soap formation, which could make separation difficult, and copper salts were removed by

precipitation with Na_2S. The general procedure was as follows. A round-bottom flask containing a stir bar was flame dried, and the flask was allowed to cool to room temperature and then flushed with nitrogen. 11-Bromoundecanoic acid (2 g, 7.54 mmol) was measured into the flask, which was covered with a septum and flushed with nitrogen to ensure dryness and to remove air. THF (9.4 mL) was added, and the stirred solution was cooled in an ethanol bath maintained at −20 to −25 °C by the addition of dry ice. The appropriate Grignard reagent (1.0 equiv, e.g., 3.8 mL of a 2.0 M solution) was then introduced dropwise. Lithium tetrachlorocuprate (1.5 mL of a 0.1 M solution in THF, 0.15 mmol, 0.02 equiv) was added, followed by another 1.025 equiv of Grignard reagent. The reaction mixture was stored in a −20 °C freezer overnight. An aliquot (0.5 μL) of the reaction was withdrawn and analyzed by GC/MS for the presence of unreacted bromoacid. Additional portions of Grignard agent were added as needed and allowed to react for at least 4 h each until the starting material was completely consumed.

The reaction mixture was transferred into a separatory funnel, quenched cautiously with 25 mL of 1 M H_2SO_4 and 50 mL of toluene. The lower aqueous layer was confirmed to be acidic using litmus paper and was removed. The organic layer was extracted with 25 mL of 0.1 M H_2SO_4, and then with water containing a slight excess of sodium sulfide with respect to copper, causing black specks of copper sulfide to drop to the bottom of the funnel. The bottom layer was collected into another separatory funnel and back-extracted with 10 mL of toluene. All organic layers were combined and concentrated by rotary evaporation, and the product was purified by bulb-to-bulb distillation under vacuum. The purified products were analyzed by GC/MS (after methylation) and ^{1}H NMR spectroscopy to confirm identity and purity. ^{1}H NMR results matched literature values published by Richardson and Williams.[75]

13-methyltetradecanoic acid (i-15:0): from 2.01 g of 11-bromoundecanoic and isobutylmagnesium chloride was obtained 1.70 g (93 %) of the product as a white solid (98% purity by GC/MS). ^{1}H NMR (400 MHz, $CDCl_3$): δ (ppm) 0.83 (d, 6H, J = 6.6 Hz), 1.16–1.08 (m, 2H), 1.35–1.16 (m, 16H), 1.49 (1H, m), 1.59 (2H, p, J = 7.0 Hz), 2.3 (t, 2H, J = 7.4 Hz), 8.67 (br s, 1H).

14-Methylpentadecanoic acid (i-16:0): From 2.0 g of 11-bromoundecanoic and isopentylmagnesium bromide was obtained 1.21 g (62%) of the product as a white solid (88% purity by GC/MS). ^{1}H NMR (400 MHz, $CDCl_3$): δ (ppm) 0.84 (d, 6H, J = 6.6 Hz), 1.14 (p, 2H, J = 6.7 Hz), 1.35–1.19 (m, 18H), 1.56–1.35 (m, 2H), 1.61 (p, 2H, J = 7.4 Hz), 2.33 (t, 2H, J = 7.69 Hz).

Synthesis of Phospholipids

Intermediates in the synthesis of the proposed chimeric phospholipids were synthesized using the approach described by Lindberg et al. for the synthesis of phosphatidic acids.[71] The first step in this route is the synthesis of a protected phosphate ester. The product has the (*R*)-configuration due to a priority change in the substituents of the *sn*-2 carbon.

*Step 1: Synthesis of (R)-di-tert-butyl-phosphonoglycidol (**6**)*

(*S*)-glycidol (233 mg, 3.21 mmol) was added to 1.58 g (5.70 mmol, 1.78 equiv) of di-*tert*-butyl *N,N*-diisopropylphosphoramidite in a dried round bottom flask sealed with a septum. DCM (100 mL) was introduced, followed by dropwise addition of 1*H*-tetrazole solution (0.45 M in acetonitrile, 24.2 mL, 10.9 mmol, 3.4 equiv). After 30 min, the solution was cooled to 0 °C, and *m*-CPBA (ca. 70% purity,1.70 g, ca 7 mmol, ca 4 equiv with respect to phosphorus) was added. The reaction mixture was stirred for 40 min and transferred into a separatory funnel with the aid of 10 mL of DCM followed by 10 mL of 10% aqueous $Na_2S_2O_3$ to reduce excess *m*-CPBA. The

aqueous layer was extracted with an additional 10 mL of DCM, and the combined organic layers were washed with 10 mL of $NaHCO_3$, dried over sodium sulfate, concentrated using a rotary evaporator and stored at −20 °C. The product was purified by flash chromatography on a 25 × 150 mm bed of silica gel eluted with 150-mL portions each of 2:1, 1:1 and then 1:1.5 hexane:ethyl acetate containing 1% triethylamine. Evaporation of the solvent under reduced pressure afforded the product as a colorless oil (92 mg, 35%) TLC (silica gel, F_{254}, hexane:EtOAc 1:1 with 1% Et_3N): R_f 0.37. ^1H NMR data matched those reported by Lindberg et al.[72]

Step 2: Regioselective Epoxide Ring-Opening by Cesium Palmitate

Synthesis of cesium palmitate. The cesium palmitate required for this step was synthesized from palmitic acid and cesium carbonate.[76] To 325mg (0.997 mmol) of Cs_2CO_3 in 10 mL of CH_3OH was added 770 mg (3.00 mmol, 3.0 equiv) of palmitic acid, and the solution was warmed while stirring to 40 °C for 40 min. The reaction mixture was cooled to room temperature, methanol was removed by rotary evaporation, and ether (45 mL) was introduced to dissolve excess palmitic acid. The product was collected by vacuum filtration and washed with ether to yield 521 mg (67%) of cesium palmitate.

Synthesis of 3-O,O-di-tert-butylphosphono-1-O-palmitoyl-sn-glycerol (7). Cesium palmitate (197 mg, 0.51 mmol, 3.0 equiv) was added to 45 mg (0.17 mmol) of (*R*)-di-*tert*-butylphosphonoglycidol in a 25-ml round bottom flask containing a stirring bar. Palmitic acid (43 mg, 0.17 mmol, 1.0 equiv) and 1.7 mL of DMF were added, and the mixture was heated at 80 °C for 10 h in an oil bath. The reaction was cooled to room temperature, then transferred with the aid of 45 mL of diethyl ether into a 100 mL flask and concentrated under reduced pressure. To remove DMF, 45 mL of toluene was added, and the volatiles were removed by rotary

evaporation. Chloroform was added, the precipitate was filtered off, and the sample was concentrated by drying under nitrogen to obtain 152 mg (57%) of the crude product. Chromatographic purification was carried out on small scale with 32 mg of the sample using a Pasteur pipette packed with silica gel to remove traces of palmitic acid. The product was eluted with 8 mL of 2:1 and 5 ml of 3:1 toluene:ethyl acetate containing 1% triethylamine. Evaporation of the solvent gave 12 mg (38%) of the product; however, traces of palmitic acid were still observed in the ^{1}H NMR spectrum. ^{1}H NMR data matched those reported by Lindberg et al.[72]

CHAPTER 3. RESULTS AND DISCUSSION

Fluidity as a Function of Temperature in POPC Vesicles

Vesicle fluidity at different temperatures were analyzed using Laurdan fluorescence (Figure 18). As earlier indicated, Laurdan is capable of sensing differences in fluidity in membranes, and it shows emission maxima of 440 nm and 490 nm in ordered and disordered membrane environments, respectively.[52]

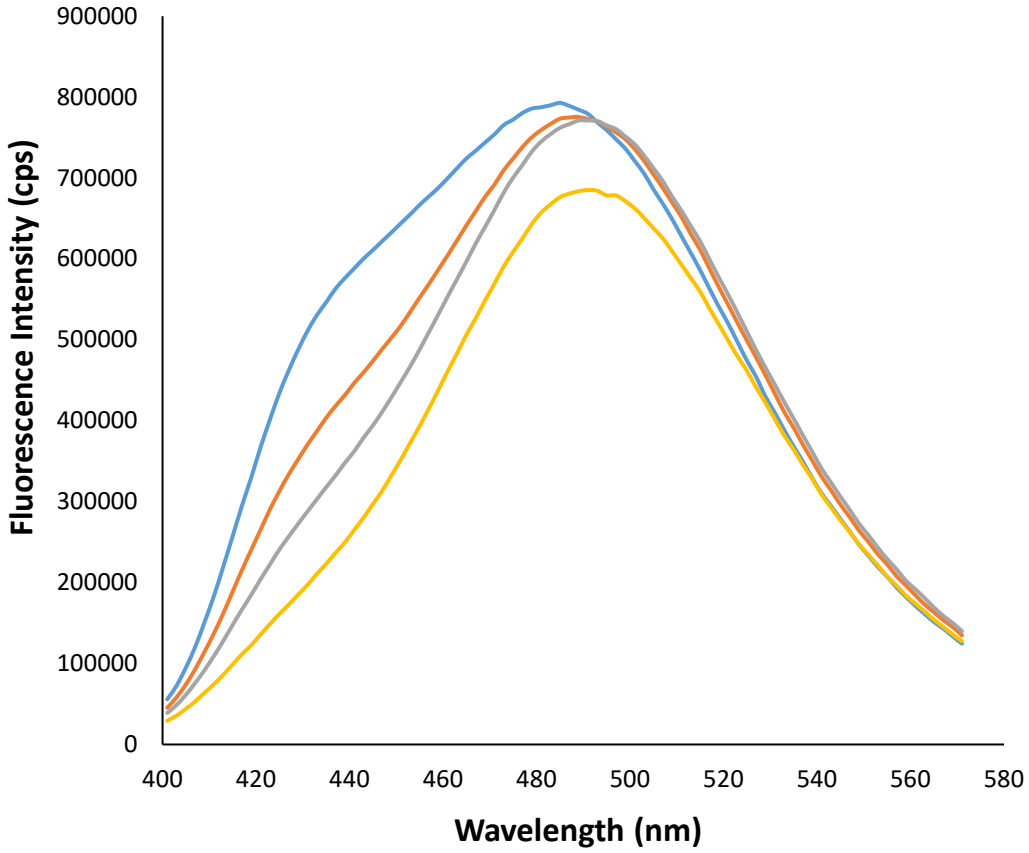

Figure 18. Fluorescence spectra of Laurdan in 1-palmitoyl-2-oleoyl-*sn*-glycero-3-phosphocholine (POPC) vesicles as a function of temperature. Blue, orange, grey and yellow lines are plots at temperatures of 20, 29.5, 37.7 and 48.8 ℃, respectively

The fluorescence spectra of Laurdan in POPC vesicles at 20 ℃ showed a small peak near 440 and a larger one near 490 nm, reflecting a substantially fluid bilayer (Figure 18). As the

temperature was increased from 20 ℃ the peak near 440 nm weakened progressively until it disappeared at the highest temperature studied, 48.8 ℃, consistent with fluidization of the bilayer[50] This qualitative trend is supported by a progressive decrease in the GP value with increasing temperature (Figure 19).[52,53] These results demonstrate that POPC vesicles display the expected temperature dependence on fluidity, and that Laurdan is a useful probe for future work.

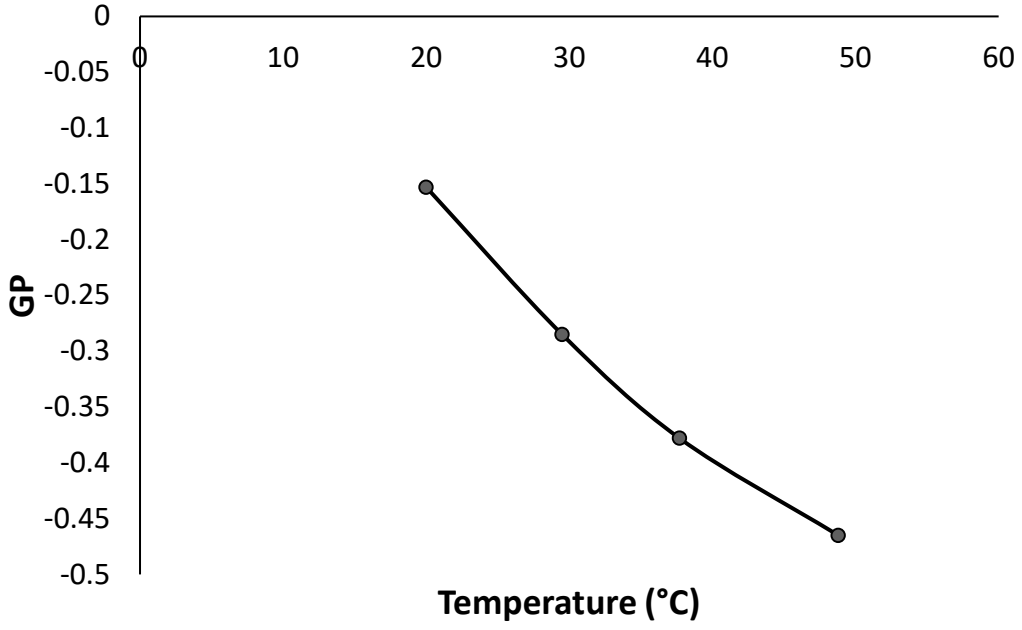

Figure 19. General polarization (GP) as a function of temperature for Laurdan in POPC unilamellar vesicles. GP was calculated at temperatures 20, 29.5, 37.7 and 48.8 ℃ from emission intensities at 440 and 490 nm

Synthesis of 12-Bromododecanoic Acid

12-bromododecanoic acid was needed as a precursor for the synthesis of C_{17} branched-chain fatty acids from commercially available Grignard reagents. It was synthesized in a single step from commercial 12-hydroxydodecanoic acid and concentrated hydrobromic acid at reflux. These conditions afforded the product in 85% yield, or 80% after recrystallization. The identity and purity of the compound were confirmed by GC/MS and NMR (Figure 20).

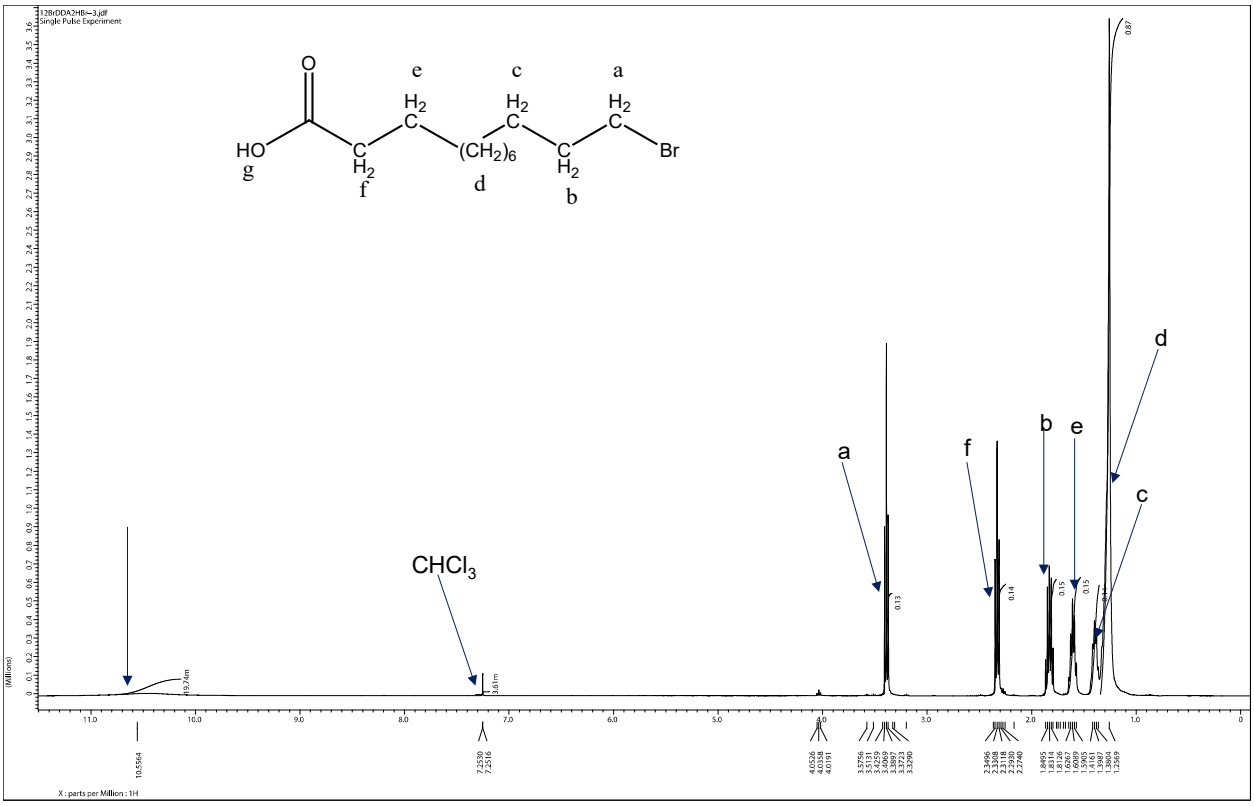

Figure 20. ^{1}H NMR spectrum and assignments of 12-bromododecanoic acid

For GC/MS, 12-bromododecanoic acid was derivatized by silylation rather than methylation because partial replacement of bromine with chlorine was observed in GC/MS when methylation with HCl/methanol was used for derivatization.

A second synthetic route for synthesizing 12-bromododecanoic acid was also carried out by using H_2SO_4 (as acid co-catalyst) and HBr. This procedure gave only a 32% yield, which is a substantially lower yield than was attained by using HBr alone.

GC/MS Analysis of 12-Bromododecanoic Acid Methyl Ester

Analysis of the 12-bromododecanoic acid as its FAME derivative showed the expected product at a retention time of 11.95 min. In the mass spectrum (Figure 21), a weak molecular ion

was observed, with peaks of equal intensity at *m/z* 292 and 294 reflecting the equal abundance of ^{79}Br and ^{81}Br, along with expected fragments at 261/263 (loss of methoxyl) and 213 (loss of Br).

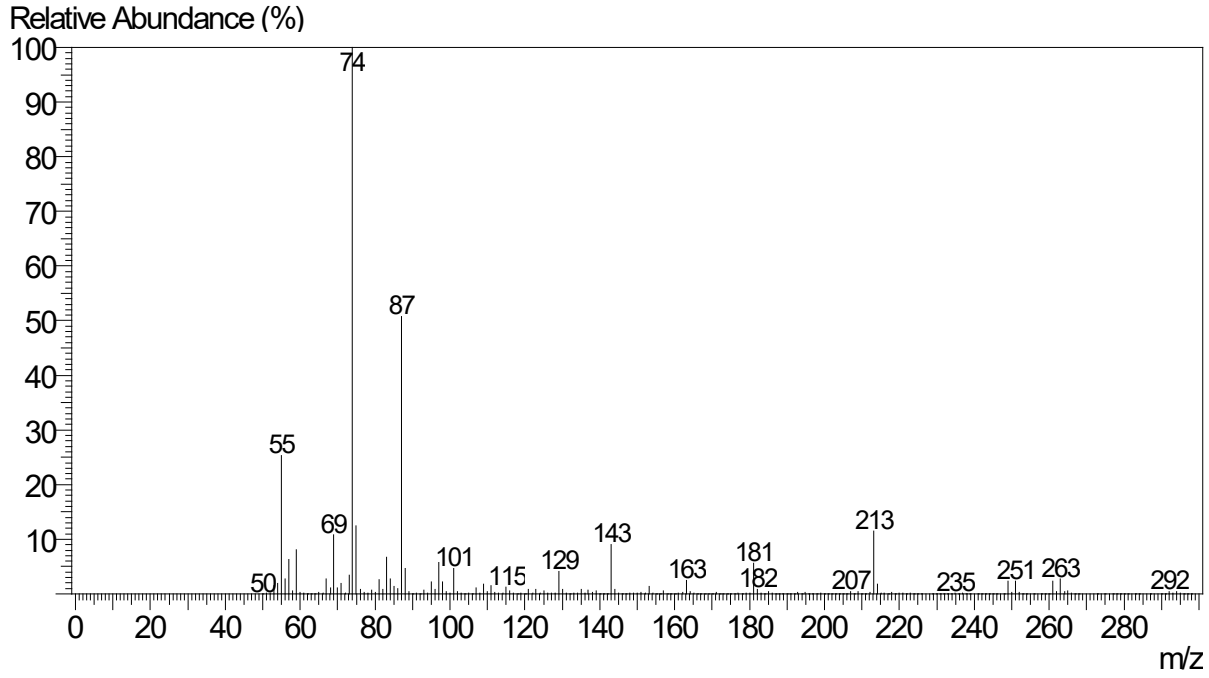

Figure 21. Electron-impact mass spectrum of 12-bromododecanoic acid methyl ester. MS(EI): *m/z* 292/294 (1/1, M+), 261/263 (3/3, M−OCH_3), 213 (12, M−Br), 143 (10, $C_8H_{15}O_2$), 87 (52, $C_4H_7O_2$), 74 (100, $C_3H_5O_2$)

A significant impurity peak representing approximately 35% of the product was observed at a retention time of 11.43 min. The mass spectrum of this compound was very similar to that of the expected product but lacked the molecular ion. Close examination of the spectrum led to the identification of this impurity as 12-chlorododecanoic acid methyl ester, produced as an artifact of derivatization (Figure 22). The mass spectrum similarly displayed a weak molecular ion peak at m/z 248 and 250, with intensities in the characteristic 3:1 ratio of ^{35}Cl to ^{37}Cl, and similar fragment ions at 217/219 (loss of methoxyl) and 213 (loss of Cl).

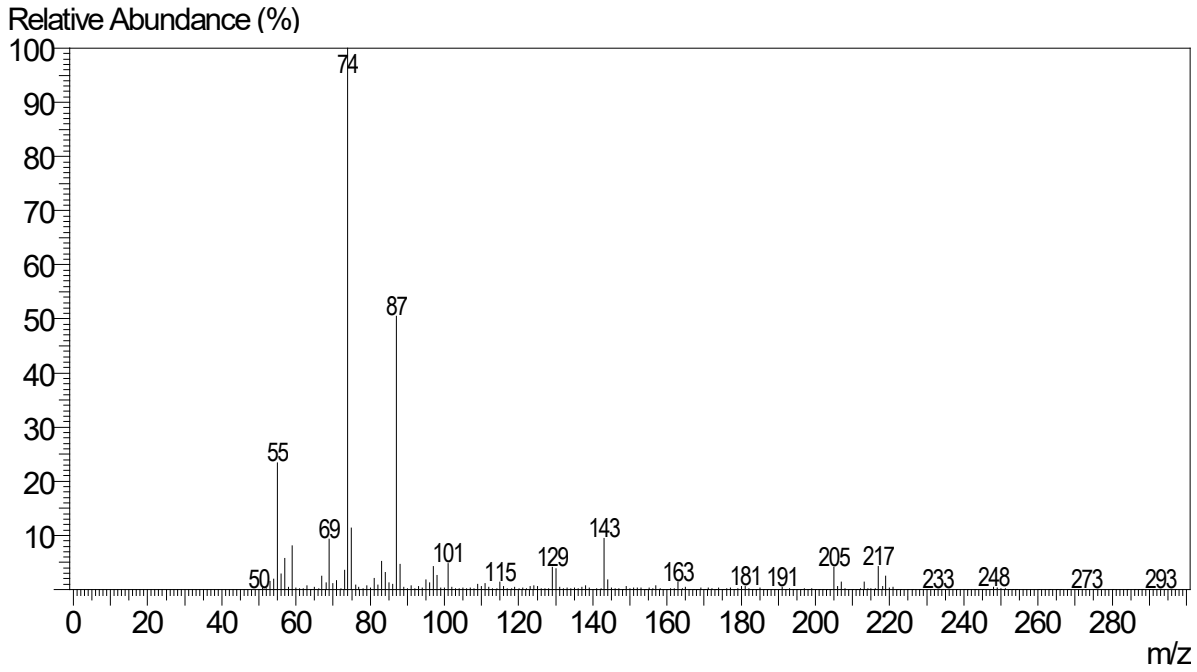

Figure 22. Electron-impact mass spectrum of 12-chlorododecanoic acid methyl ester. MS(EI): *m*/*z* 248/250 (1%/~0.3%, M+), 233/235 (1/~0.3, M−CH_3), 217/219 (3/1, M−OCH_3), 233 (1, M−Cl).

Synthesis of Fatty Acids

Fatty acids are readily synthesized from ω-bromocarboxylic acids and Grignard reagents under the influence of a copper catalyst (Figure 23).[75] Grignard reagents are strong bases, and as a result, the first equivalent of Grignard reagent added in the reaction deprotonates the acidic proton of the bromoacid to form a magnesium carboxylate salt.[77] At low temperature, nucleophilic addition of the Grignard to the carboxylate ion is slow, and deprotonation effectively protects the carboxyl group from addition. The second equivalent of Grignard reagent at −20 °C displaces bromine in the presence of lithium tetrachlorocuprate (Li_2CuCl_4) as a catalyst.[78] The reaction is carried out in THF, an apolar protic solvent in which Grignard reagents, magnesium carboxylates and Li_2CuCl_4 are adequately soluble at −20 °C. Due to the

sensitivity of Grignard reagents to air and water, reactions were conducted under a nitrogen atmosphere.

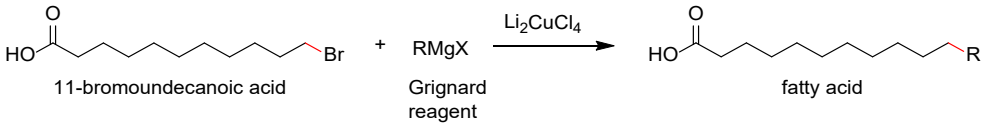

Figure 23. Approach to the synthesis of branched-chain fatty acids from 11-bromododecanoic acid and Grignard reagents

The synthesis of fatty acids from Grignard reagents and ω-haloacids (e.g 11-bromododecanoic acid) is one of the most effective synthetic routes, with product yields up to 94% reported.[74] In this research, two fatty acids were synthesized from 11-bromoundecanoic acid in yields of 62 and 93% (Table 1), consistent with the published results. The lower yield of 14-methylpentadecanoic acid (i-16:0) obtained was most likely a result of the losses that occurred during isolation by extraction.

Table 1. Summary of Fatty Acid Synthesis

Fatty acid	**Grignard Reagent**	**Mass of undecanoic acid used (g)**	**Mass of Product (g)**	**% Yield**	**% Purity**
i-16:0	isopentylmagnesium bromide	2.00	1.21	62	88
i-15:0	isobutylmagnesium chloride	2.01	1.70	93	98

Analysis of the fatty acids was initially performed with GC/MS, both during the reaction and after purification. For this purpose, the fatty acids were converted to their methyl ester (fatty acid methyl ester or FAME) derivatives using HCl/methanol (Figure 24). A representative chromatogram is shown in Figure 28 for 13-methyltetradecanic acid (*i*-15:0) FAME. The chromatogram shows complete consumption of the bromoacid precursor and a single peak at

11.27 min, with a mass spectrum matching the standard spectrum in the library on the instrument (Figure 25). Purity of the 14-methyl pentadecanoic acid (i-16:0) assessed by this method was 88% (chromatogram provided in Appendix B1). ^{1}H NMR spectroscopy showed that *i*-15:0 had impurities recognized by unexpected peaks at δ 0.8 and 3.4 ppm (Appendix C1), and *i*-16:0 had impurities recognized by unexpected peaks at δ 0.9, 3.6 and 4.0 ppm (Appendix B3). Recrystallization of the impure i-15:0 from hexane substantially reduced the level of the impurity (Figures 26 and 27). However, the recrystallized i-16:0 still showed the impurity at 0.9 ppm (Appendix B4).

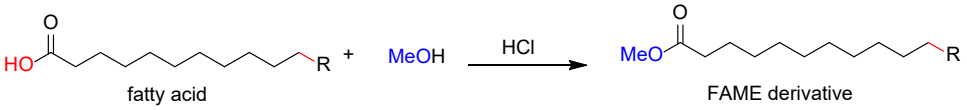

Figure 24. Derivatization of fatty acids as their methyl esters (FAMEs)

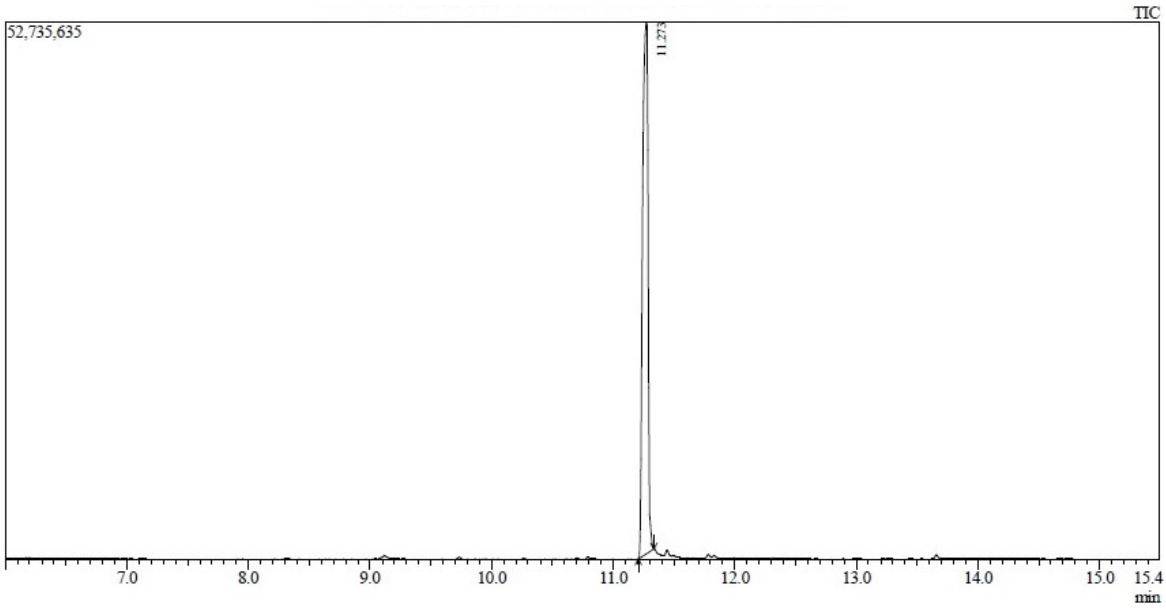

Figure 25. GC/MS total ion chromatogram of 13-methyltetradecanoic acid (i-15:0) methyl ester

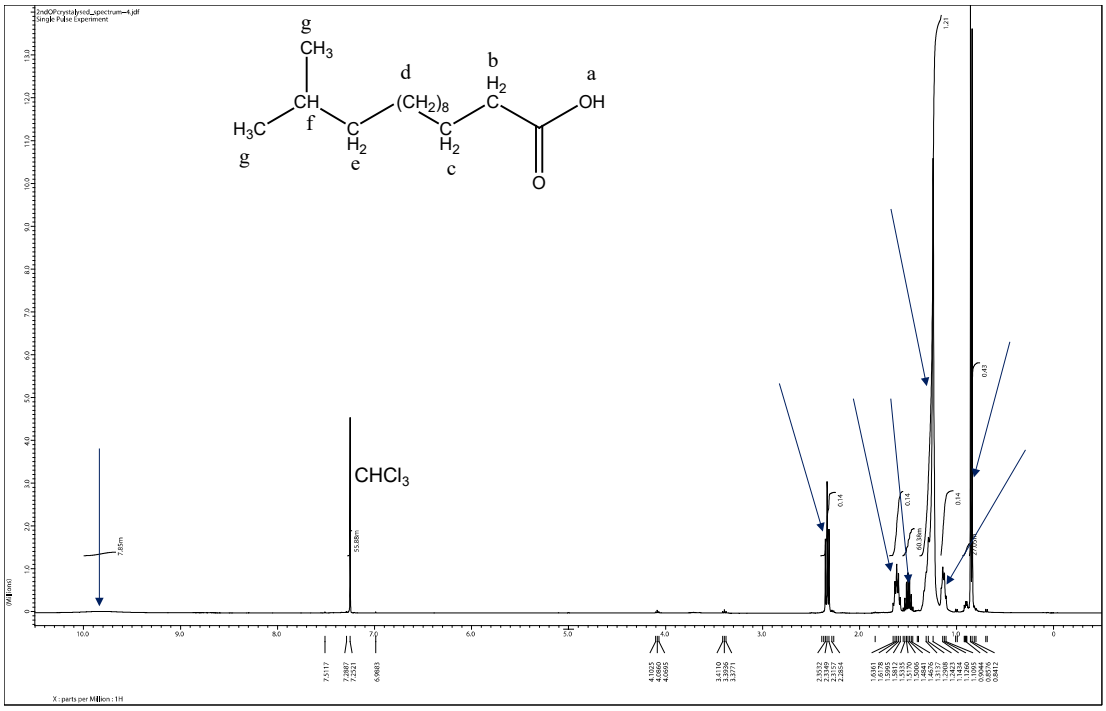

Figure 26. ^{1}H NMR spectrum and assignments of 13-methyltetradecanoic acid (i-15:0)

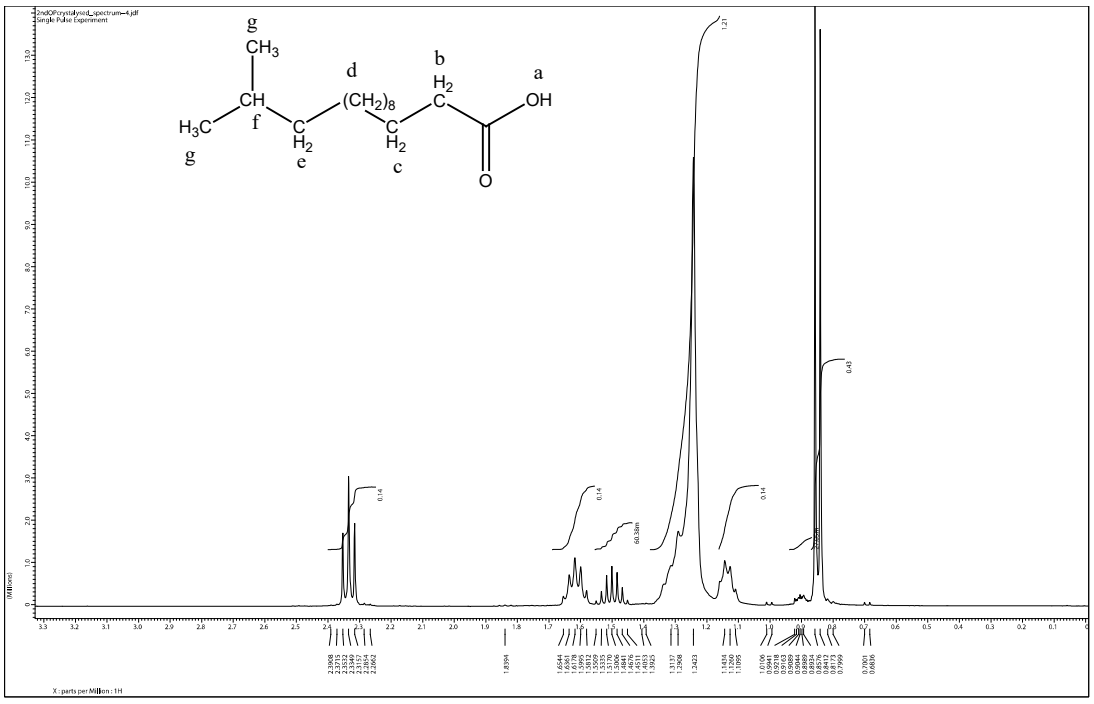

Figure 27. ^{1}H NMR spectrum and assignments of 13-methyltetradecanoic acid (i-15:0), scale expansion

Synthesis of Phospholipids

With the synthesis of two bacterial branched-chain fatty acids completed, efforts toward their incorporation into PC lipids was commenced according to the plan illustrated in Figure 18. The first step on the route was installation of a protected phosphate moiety at the *sn*-3 position of glycerol. For this purpose, (*S*)-glycidol (**4**) was reacted with di-*tert*-butyl-*N*,*N*-diisopropylphosphoramidite (**1**) in the presence of 1H-tetrazole (**2**), commonly used as an activator for phosphoramidites. It has a dual function of protonating the amino group of the phosphoramidite to make it a good leaving group, and also acting as a nucleophilic catalyst to displace the diisopropylamino group to form tetrazolide intermediate (**3**).[79] The tetrazolide intermediate undergoes nucleophilic attack by (*S*)-glycidol (**4**) to form a phosphite ester (**5**), which is oxidized *in situ* with *m*-CPBA to the corresponding phosphate (**6**) (Figure 28). The synthesized product was purified by flash column chromatograph and analyzed by ^{1}H NMR spectroscopy to confirm its identity and purity (Figure 29). The NMR spectrum corresponds with literature result.[71]

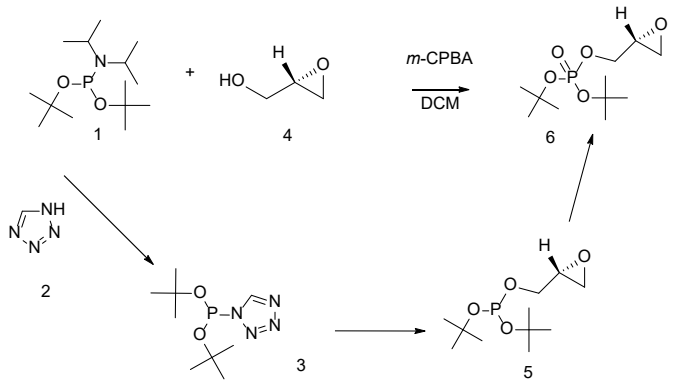

Figure 28. Reaction scheme for the phosphorylation of (*S*)-glycidol

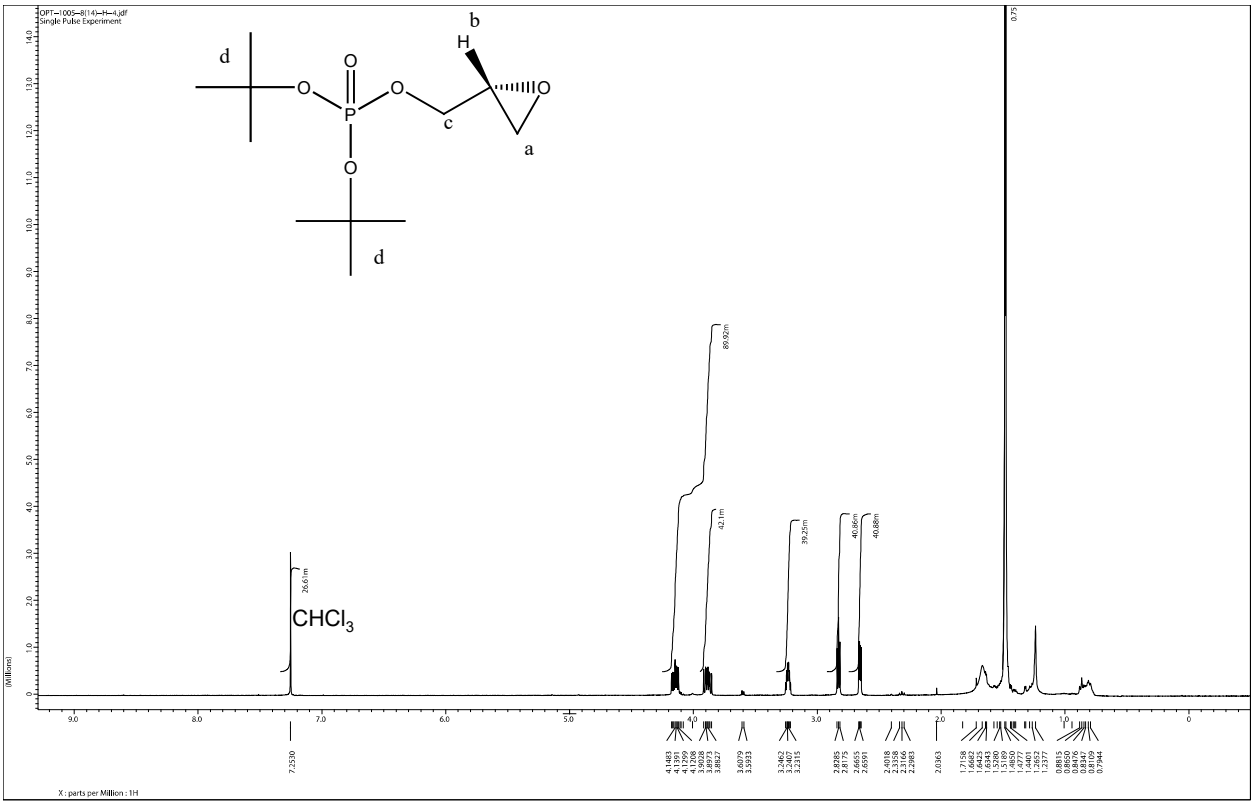

Figure 29. ^{1}H NMR spectrum of (*R*)-di-*tert*-butylphosphonoglycidol (phosphate ester **6**)

The second step in the synthesis was to install the *sn*-1 fatty acid regioselectively. For this purpose, cesium palmitate used was required. It was synthesized from palmitic acid and cesium carbonate as described in Chapter 2 and used without further purification (Figure 30).

$$\underset{\text{cesium carbonate}}{Cs_2CO_3} + \underset{\text{palmitic acid}}{2\ C_{15}H_{31}COOH} \xrightarrow[40\ ^\circ C]{CH_3OH} \underset{\text{cesium palmitate}}{2\ C_{15}H_{31}COOCs} + \underset{\text{carbon dioxide}}{CO_2} + \underset{\text{water}}{H_2O}$$

Figure 30. Synthesis of cesium palmitate

Reaction of the cesium palmitate with the phosphorylated glycidol (phosphate ester **6**) in DMF at 80 °C led to regioselective nucleophilic opening of the epoxide ring to afford the protected lyso-phosphatidic acid 3-*O*,*O*-di-*tert*-butylphosphono-1-*O*-palmitoyl-*sn*-glycerol (**7**)

(Figure 31). ^{1}H NMR analysis of the crude product revealed it to be substantially pure, with the only significant impurity being excess palmitic acid from the reaction, and peaks matching the reported data.[71] ^{1}H NMR also showed that the use of toluene to remove residual DMF from the product was successful (figure 32). The excess palmitic acid was removed by flash chromatography performed in a Pasteur pipet. Time did not permit further progress, and completion of the synthesis is left for future work.

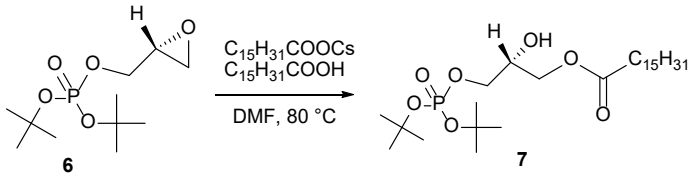

Figure 31. Synthesis of 3-*O,O*-di-*tert*-butylphosphono-1-*O*-palmitoyl-*sn*-glycerol

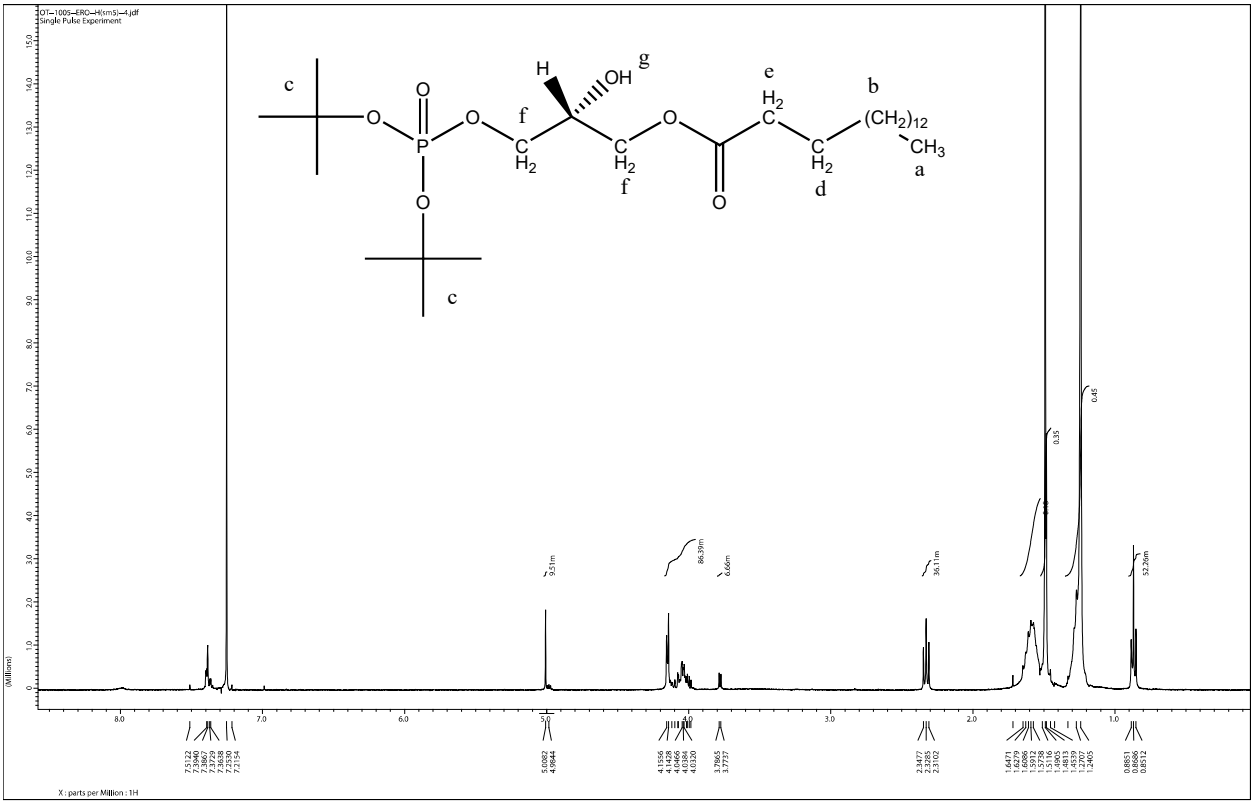

Figure 32. ^{1}H NMR spectrum of 3-*O*,*O*-di-*tert*-butylphosphono-1-*O*-palmitoyl-*sn*-glycerol

CHAPTER 4. CONCLUSIONS AND FUTURE RESEACRH

Understanding and mitigating the toxicity of solvents and biofuels to producer organisms remains a critical barrier in the production of advanced biofuels. Toward that end, I undertook the creation of new membrane models for *B. subtilis*, a biotechnologically relevant organism. Specifically, I targeted the synthesis of novel, chimeric phospholipids bearing bacterial fatty acids and a eukaryotic head group, phosphocholine, to study how they were affected by fuels and solvents.

In pilot experiments, I prepared Laurdan-doped unilamellar vesicles from POPC and successfully obtained fluorescence general polarization (GP) values consistent with the expectation that the vesicles became increasingly fluid as temperature was increased. These experiments showed the utility of Laurdan GP measurements for future work.

Subsequently, I undertook the synthesis of two branched-chain fatty acids common in *B. subtilis*. These were made using a copper-catalyzed Grignard substitution of 11-bromoundecanoic acid. The synthesized fatty acids were purified by bulb-to-bulb vacuum distillation and analyzed by GC/MS and ^{1}H NMR to confirm purity and identity. The percentage yield of synthesized fatty acids *i*-15:0 and *i*-14:0 were 62% and 93% respectively, but the *i*-15:0 still had minor impurities even after purification by recrystallization from hexane.

Finally, I initiated the synthesis of chimeric phospholipids using the strategy of Lindberg et al.[71] to construct the phosphatidic acid moiety. The first two steps were successfully performed, leading to palmitoyl lyso-phosphatidic acid with *tert*-butyl protecting groups on the phosphate moiety, although the yield was lower than expected for the first step.

For future research, there are several goals. First, C_{17} fatty acids will be prepared using the synthesized 12-bromododecanoic acid. Next, the synthesis of chimeric phospholipids will be

completed. In the first example, a-15:0 will be coupled to 3-*O*,*O*-di-tert-butylphosphono-1-*O*-palmitoyl-*sn*-glycerol using DCC and DMAP to synthesize a protected phosphatidic acid, as explained by Lindberg et al. After removal of the *tert*-butyl protecting groups, the phosphocholine head group will be introduced using triisopropyl benzenesulfonyl chloride and choline tetraphenylborate as described by Harbison and Griffin.[80] Several other examples bearing different bacterial fatty acids at the *sn*-2 position will be synthesized. Finally, the chimeric phospholipids will be used to make model membranes, and the effects of relevant solvents (e.g., THF, butanol and ethanol) will be studied at several temperatures using Laurdan fluorescence general polarization. In this way, an understanding of how PC heads interact with bacterial tails in the context of solvent disruption will be obtained, and in the best case, a composition displaying superior fuel-resistance will be obtained.

REFERENCES

1. Dunlop, M. J. Engineering Microbes for Tolerance to Next-Generation Biofuels. *Biotechnol. Biofuels* **2011**, *4* (1), 32. https://doi.org/10.1186/1754-6834-4-32

2. Huffer, S.; Clark, M. E.; Ning, J. C.; Blanch, H. W.; Clark, D. S. Role of Alcohols in Growth, Lipid Composition, and Membrane Fluidity of Yeasts, Bacteria, and Archaea. *Appl. Environ. Microbiol.* **2011**, *77* (18), 6400–6408. https://doi.org/10.1128/AEM.00694-11

3. Heipieper, H. J.; Bont, J. a M. De. Adaptation of Pseudomonas Putida S12. *Appl. Environ. Microbiol.* **1994**, *60* (12), 4440–4444. https://doi.org/10.1128/aem.60.12.4440-4444.1994

4. Petitdemange, H. Regulation and Butanol Inhibition of D-Xylose. *Appl. Environ. Microbiol* **1985**, *49* (4), 874–878. https://doi.org/10.1128/aem.49.4.874-878.1985

5. Vollherbst Schneck, K.; Sands, J. A.; Montenecourt, B. S. Effect of Butanol on Lipid Composition and Fluidity of Clostridium Acetobutylicum ATCC 824. *Appl. Environ. Microbiol.* **1984**, *47* (1), 193–194. https://doi.org/10.1128/aem.47.1.193-194.1984

6. Fonseca, F.; Pénicaud, C.; Tymczyszyn, E. E.; Gómez-Zavaglia, A.; Passot, S. Factors Influencing the Membrane Fluidity and the Impact on Production of Lactic Acid Bacteria Starters. *Appl. Microbiol. Biotechnol.* **2019**, *103* (17), 6867–6883. https://doi.org/10.1007/s00253-019-10002-1

7. Halder, P.; Azad, K.; Shah, S.; Sarker, E. Prospects and Technological Advancement of Cellulosic Bioethanol Ecofuel Production. *Adv. Eco-Fuels a Sustain. Environ.* **2019**, No. February, 211–236. https://doi.org/10.1016/b978-0-08-102728-8.00008-5

8. Halder, P. K.; Paul, N.; Joardder, M. U. H.; Sarker, M. Energy Scarcity and Potential of Renewable Energy in Bangladesh. *Renew. Sustain. Energy Rev.* **2015**, *51*, 1636–1649. https://doi.org/10.1016/j.rser.2015.07.069

9. Du, C.; Zhao, X.; Liu, D.; Lin, C. S. K.; Wilson, K.; Luque, R.; Clark, J. Introduction: An Overview of Biofuels and Production Technologies. An Overview of Biofuels and Production Technologies. In *Handbook of Biofuels Production: Processes and Technologies: Second Edition*; Rafael Luque, , Carol Sze Ki Lin, , Karen Wilson, , James Clark, and K. W., Ed.; Elsevier Science & Technology, **2016**; pp 3–12. https://doi.org/10.1016/B978-0-08-100455-5.00001-1

10. Elshahed, M. S. Microbiological Aspects of Biofuel Production: Current Status and Future Directions. *J. Adv. Res.* **2010**, *1* (2), 103–111. https://doi.org/10.1016/j.jare.2010.03.001

11. Tarr, T. E. D.; Fuels, A.; West, G. Ethanol in Motor Gasoline. In *Monohydric alcohols*; Wickson, E. J., Ed.; American Chemical Society, **1981**; Vol. 159, pp 55–70. https://doi.org/DOI: 10.1021/bk-1981-0159.ch005

12. Goldemberg, J.; Coelho, S. T.; Nastari, P. M.; Lucon, O. Ethanol Learning Curve - The Brazilian Experience. *Biomass and Bioenergy* **2004**, *26* (3), 301–304. https://doi.org/10.1016/S0961-9534(03)00125-9

13. Fischer, C. R.; Klein-Marcuschamer, D.; Stephanopoulos, G. Selection and Optimization of Microbial Hosts for Biofuels Production. *Metab. Eng.* **2008**, *10* (6), 295–304. https://doi.org/10.1016/j.ymben.2008.06.009

14. Smith, M. D. An Abbreviated Historical and Structural Introduction to Lignocellulose. *ACS Symp. Ser.* **2019**, *1338*, 1–15. https://doi.org/10.1021/bk-2019-1338.ch001

15. Saha, B. C. Lignocellulose Biodegradation and Applications in Biotechnology. In *Lignocellulose Biodegradation*; American Chemical Society, **2004**; Vol. 889, pp 2–34. https://doi.org/10.1021/bk-2004-0889.ch001

16. Hayes, M. H. B.; Mylotte, R.; Swift, R. S. *Humin: Its Composition and Importance in Soil Organic Matter*, 1st ed.; Elsevier Inc., **2017**; Vol. 143. https://doi.org/10.1016/bs.agron.2017.01.001

17. Kumar, R.; Tabatabaei, M.; Karimi, K.; Horváth, I. S. Recent Updates on Lignocellulosic Biomass Derived Ethanol - A Review. *Biofuel Res. J.* **2016**, *3* (1), 347–356. https://doi.org/10.18331/BRJ2016.3.1.4

18. Mielenz, J. R. *Small-Scale Approaches for Evaluating Biomass Bioconversion for Fuels and Chemicals*, Second Edi.; Elsevier, **2020**. https://doi.org/10.1016/b978-0-12-815497-7.00027-0

19. Li, J.; Zhang, W.; Xu, S.; Hu, C. The Roles of H_2O/Tetrahydrofuran System in Lignocellulose Valorization. *Front. Chem.* **2020**, *8* (February). https://doi.org/10.3389/fchem.2020.00070

20. Pingali, S. V.; Smith, M. D.; Liu, S. H.; Rawal, T. B.; Pu, Y.; Shah, R.; Evans, B. R.; Urban, V. S.; Davison, B. H.; Cai, C. M.; Ragauskas, A. J.; O'Neill, H. M.; Smith, J. C.; Petridis, L. Deconstruction of Biomass Enabled by Local Demixing of Cosolvents at Cellulose and Lignin Surfaces. *Proc. Natl. Acad. Sci. U. S. A.* **2020**, *117* (29), 16776–16781. https://doi.org/10.1073/pnas.1922883117

21. Cray, J. A.; Stevenson, A.; Ball, P.; Bankar, S. B.; Eleutherio, E. C. A.; Ezeji, T. C.; Singhal, R. S.; Thevelein, J. M.; Timson, D. J.; Hallsworth, J. E. Chaotropicity: A Key Factor in Product Tolerance of Biofuel-Producing Microorganisms. *Curr. Opin. Biotechnol.* **2015**, *33* (Box 1), 228–259. https://doi.org/10.1016/j.copbio.2015.02.010

22. Dunlop, M. J. Engineering Microbes for Tolerance to Next-Generation Biofuels. *Biotechnol. Biofuels* **2011**, *4* (1), 32. https://doi.org/10.1186/1754-6834-4-32

23. Nickels, J. D.; Chatterjee, S.; Mostofian, B.; Stanley, C. B.; Ohl, M.; Zolnierczuk, P.; Schulz, R.; Myles, D. A. A.; Standaert, R. F.; Elkins, J. G.; Cheng, X.; Katsaras, J. *Bacillus*

Subtilis Lipid Extract, A Branched-Chain Fatty Acid Model Membrane. *J. Phys. Chem. Lett.* **2017**, *8* (17), 4214–4217. https://doi.org/10.1021/acs.jpclett.7b01877

24. Silhavy, T. J.; Kahne, D.; Walker, S. The Bacterial Cell Envelope. *Cold Spring Harb. Perspect. Biol.* **2010**, *2* (5). https://doi.org/10.1101/cshperspect.a000414

25. Singer, S. J.; Nicolson, G. L. The Fluid Mosaic Model of the Structure of Cell Membranes. *Science* **1972**, *175* (4023), 720–731. https://doi.org/10.1126/science.175.4023.720

26. Nicolson, G. L. The Fluid - Mosaic Model of Membrane Structure: Still Relevant to Understanding the Structure, Function and Dynamics of Biological Membranes after More than 40 Years. *Biochim. Biophys. Acta - Biomembr.* **2014**, *1838* (6), 1451–1466. https://doi.org/10.1016/j.bbamem.2013.10.019

27. Vanounou, S.; Parola, A. H.; Fishov, I. Phosphatidylethanolamine and Phosphatidylglycerol are Segregated into Different Domains in Bacterial Membrane. A Study with Pyrene-Labelled Phospholipids. *Mol. Microbiol.* **2003**, *49* (4), 1067–1079. https://doi.org/10.1046/j.1365-2958.2003.03614.x

28. Lingwood, D.; Simons, K. Lipid Rafts as a Membrane-Organizing Principle. *Science* **2010**, *327* (5961), 46–50. https://doi.org/10.1126/science.1174621

29. López, D.; Kolter, R. Functional Microdomains in Bacterial Membranes. *Genes Dev.* **2010**, *24* (17), 1893–1902. https://doi.org/10.1101/gad.1945010

30. Bach, J. N.; Bramkamp, M. Flotillins Functionally Organize the Bacterial Membrane. *Mol. Microbiol.* **2013**, *88* (6), 1205–1217. https://doi.org/10.1111/mmi.12252

31. Rossy, J.; Ma, Y.; Gaus, K. The Organisation of the Cell Membrane: Do Proteins Rule Lipids? *Curr. Opin. Chem. Biol.* **2014**, *20* (1), 54–59. https://doi.org/10.1016/j.cbpa.2014.04.009

32. Barák, I.; Muchová, K. The Role of Lipid Domains in Bacterial Cell Processes. *Int. J. Mol. Sci.* **2013**, *14* (2), 4050–4065. https://doi.org/10.3390/ijms14024050

33. Beney, L.; Gervais, P. Influence of the Fluidity of the Membrane on the Response of Microorganisms to Environmental Stresses. *Appl. Microbiol. Biotechnol.* **2001**, *57* (1–2), 34–42. https://doi.org/10.1007/s002530100754

34. Murínová, S.; Dercová, K. Response Mechanisms of Bacterial Degraders to Environmental Contaminants on the Level of Cell Walls and Cytoplasmic Membrane. *Int. J. Microbiol.* **2014**, *2014*. https://doi.org/10.1155/2014/873081

35. Los, D. A.; Murata, N. Membrane Fluidity and Its Roles in the Perception of Environmental Signals. *Biochim. Biophys. Acta - Biomembr.* **2004**, *1666* (1–2), 142–157. https://doi.org/10.1016/j.bbamem.2004.08.002

36. Dobretsov, G. .; Borschevskaya, T. .; Petrov, V. .; Vladimirov, Y. A. The Increase of Phospholipid Bilayer Rigidity After Lipid Epoxidation. *FEBS Lett.* **1977**, *84* (1), 125–128. https://doi.org/10.1016/0014-5793(77)81071-5

37. Mansilla, M. C.; Cybulski, L. E.; Albanesi, D.; De Mendoza, D. Control of Membrane Lipid Fluidity by Molecular Thermosensors. *J. Bacteriol.* **2004**, *186* (20), 6681–6688. https://doi.org/10.1128/JB.186.20.6681-6688.2004

38. Georgiou, C. D.; Deamer, D. W. Lipids as Universal Biomarkers of Extraterrestrial Life. *Astrobiology* **2014**, *14* (6), 541–549. https://doi.org/10.1089/ast.2013.1134

39. Casares, D.; Escrib, P. V. Membrane Lipid Composition: Effect on Membrane and Organelle Structure, Function and Compartmentalization and Therapeutic Avenues. *Int. J. Mol. Sci.* **2019**, 20 (9), 2167. https://doi.org/10.3390/ijms20092167

40. Marr, A. G.; Ingraham, J. L. Effect of Temperature on the Composition of Fatty Acids in *Escherichia coli*. *J. Bacteriol*. **1962**, 84 (6), 1260–1267. https://doi.org/10.1128/jb.84.6.1260-1267.1962

41. Ingram, L. O. Adaptation of Membrane Lipids to Alcohols. *J. Bacteriol.* **1976**, *125* (2), 670–678. https://doi.org/10.1128/jb.125.2.670-678.1976

42. Huffer, S.; Clark, M. E.; Ning, J. C.; Blanch, H. W.; Clark, D. S. Role of Alcohols in Growth, Lipid Composition, and Membrane Fluidity of Yeasts, Bacteria, and Archaea. *Appl. Environ. Microbiol.* **2011**, *77* (18), 6400–6408. https://doi.org/10.1128/AEM.00694-11

43. Heipieper, H. J.; Bont, J. a M. De. Adaptation of *Pseudomonas putida* S12. *Appl. Environ. Microbiol.* **1994**, *60* (12), 4440–4444. https://doi.org/10.1128/aem.60.12.4440-4444.1994

44. Vollherbst Schneck, K.; Sands, J. A.; Montenecourt, B. S. Effect of Butanol on Lipid Composition and Fluidity of *Clostridium acetobutylicum* ATCC 824. *Appl. Environ. Microbiol.* **1984**, *47* (1), 193–194. https://doi.org/10.1128/aem.47.1.193-194.1984

45. Petitdemange, H. Regulation and Butanol Inhibition of D-Xylose. *Microbiology* **1985**, *49* (4), 874–878. https://doi.org/10.1128/aem.49.4.874-878.1985

46. Wilbanks, B.; Trinh, C. T. Comprehensive Characterization of Toxicity of Fermentative Metabolites on Microbial Growth Mike Himmel. *Biotechnol. Biofuels* **2017**, *10* (1), 1–11. https://doi.org/10.1186/s13068-017-0952-4

47. Gronenberg, L. S.; Marcheschi, R. J.; Liao, J. C. Next Generation Biofuel Engineering in Prokaryotes. *Curr. Opin. Chem. Biol.* **2013**, *17* (3), 462–471. https://doi.org/10.1016/j.cbpa.2013.03.037

48. Kwiatek, J. M.; Owen, D. M.; Abu-Siniyeh, A.; Yan, P.; Loew, L. M.; Gaus, K. Characterization of a New Series of Fluorescent Probes for Imaging Membrane Order. *PLoS One* **2013**, *8* (2), 1–7. https://doi.org/10.1371/journal.pone.0052960

49. Mazeres, S.; Joly, E.; Lopez, A.; Tardin, C. Characterization of M-Laurdan, a Versatile Probe to Explore Order in Lipid Membranes. *F1000Research* **2014**, *172*, 1–25. https://doi.org/10.12688/f1000research.4805.1

50. Weber, G.; Farris, F. J. Synthesis and Spectral Properties of a Hydrophobic Fluorescent Probe: 6-Propionyl-2-(Dimethylamino)Naphthalene. *Biochemistry* **1979**, *18* (14), 3075–3078. https://doi.org/10.1021/bi00581a025

51. Chong, P. L. G.; Wong, P. T. T. Interactions of Laurdan with Phosphatidylcholine Liposomes: A High Pressure FTIR Study. *BBA - Biomembr.* **1993**, *1149* (2), 260–266. https://doi.org/10.1016/0005-2736(93)90209-I

52. Harris, F. M.; Best, K. B.; Bell, J. D. Use of Laurdan Fluorescence Intensity and Polarization to Distinguish between Changes in Membrane Fluidity and Phospholipid Order. *Biochim. Biophys. Acta - Biomembr.* **2002**, *1565* (1), 123–128. https://doi.org/10.1016/S0005-2736(02)00514-X

53. Zhang, Y. L.; Frangos, J. A.; Chachisvilis, M. Laurdan Fluorescence Senses Mechanical Strain in the Lipid Bilayer Membrane. *Biochem. Biophys. Res. Commun.* **2006**, *347* (3), 838–841. https://doi.org/10.1016/j.bbrc.2006.06.152

54. Kobayashi, K.; Ehrlich, S. D.; Albertini, A.; Amati, G.; Andersen, K. K.; Arnaud, M.; Asai, K.; Ashikaga, S.; Aymerich, S.; Bessieres, P.; Boland, F.; Brignell, S. C.; Bron, S.; Bunai, K.; Chapuis, J.; Christiansen, L. C.; Danchin, A.; Débarbouillé, M.; Dervyn, E.; Deuerling, E.; Devine, K.; Devine, S. K.; Dreesen, O.; Errington, J.; Fillinger, S.; Foster, S. J.; Fujita, Y.; Galizzi, A.; Gardan, R.; Eschevins, C.; Fukushima, T.; Haga, K.; Harwood, C. R.; Hecker, M.; Hosoya, D.; Hullo, M. F.; Kakeshita, H.; Karamata, D.; Kasahara, Y.; Kawamura, F.; Koga, K.; Koski, P.; Kuwana, R.; Imamura, D.; Ishimaru, M.; Ishikawa, S.; Ishio, I.; le Coq, D.; Masson, A.; Mauël, C.; Meima, R.; Mellado, R. P.; Moir, A.; Moriya, S.; Nagakawa, E.; Nanamiya, H.; Nakai, S.; Nygaard, P.; Ogura, M.; Ohanan, T.; O'Reilly, M.; O'Rourke, M.; Pragai, Z.; Pooley, H. M.; Rapoport, G.; Rawlins, J. P.; Rivas, L. A.; Rivolta, C.; Sadaie, A.; Sadaie, Y.; Sarvas, M.; Sato, T.; Saxild, H. H.; Scanlan, E.; Schumann, W.; Seegers, J. F. M. L.; Sekiguchi, J.; Sekowska, A.; Séror, S. J.; Simon, M.; Stragier, P.; Studer, R.; Takamatsu, H.; Tanaka, T.; Takeuchi, M.; Thomaides, H. B.; Vagner, V.; van Dijl, J. M.; Watabe, K.; Wipat, A.; Yamamoto, H.; Yamamoto, M.; Yamamoto, Y.; Yamane, K.; Yata, K.; Yoshida, K.; Yoshikawa, H.; Zuber, U.; Ogasawara, N. Essential *Bacillus subtilis* Genes. *Proc. Natl. Acad. Sci. U. S. A.* **2003**, *100* (8), 4678–4683. https://doi.org/10.1073/pnas.0730515100

55. Nickels, J. D.; Chatterjee, S.; Stanley, C. B.; Qian, S.; Cheng, X.; Myles, D. A. A.; Standaert, R. F.; Elkins, J. G.; Katsaras, J. The in Vivo Structure of Biological Membranes and Evidence for Lipid Domains. *PLoS Biol.* **2017**, *15* (5), 1–22. https://doi.org/10.1371/journal.pbio.2002214

56. Westers, L.; Westers, H.; Quax, W. J. *Bacillus subtilis* as Cell Factory for Pharmaceutical Proteins: A Biotechnological Approach to Optimize the Host Organism. *Biochim.*

Biophys. Acta - Mol. Cell Res. **2004**, *1694* (1-3 SPEC.ISS.), 299–310. https://doi.org/10.1016/j.bbamcr.2004.02.011

57. Shafi, J.; Tian, H.; Ji, M. Bacillus Species as Versatile Weapons for Plant Pathogens: A Review. *Biotechnol. Biotechnol. Equip.* **2017**, *31* (3), 446–459. https://doi.org/10.1080/13102818.2017.1286950

58. Kaneda, T. Fatty Acids of the Genus *Bacillus*: An Example of Branched Chain Preference. *Bacteriol. Rev.* **1977**, *41* (2), 391–418. https://doi.org/10.1128/br.41.2.391-418.1977

59. Moss, C. W.; Lewis, V. J. Characterization of *Clostridia* by Gas Chromatography. I. Differentiation of Species by Cellular Fatty Acids. *Appl. Microbiol.* **1967**, *15* (2), 390–397. https://doi.org/10.1128/am.15.2.390-397.1967

60. Kämpfer, P. Limits and Possibilities of Total Fatty Acid Analysis for Classification and Identification of *Bacillus* Species. *Syst. Appl. Microbiol.* **1994**, *17* (1), 86–98. https://doi.org/10.1016/S0723-2020(11)80035-4

61. Suutari, M.; Laakso, S. Unsaturated and Branched Chain-Fatty Acids in Temperature Adaptation of *Bacillus subtilis* and *Bacillus megaterium*. *Biochim. Biophys. Acta (BBA)/Lipids Lipid Metab.* **1992**, *1126* (2), 119–124. https://doi.org/10.1016/0005-2760(92)90281-Y

62. Weber, M. H. W.; Klein, W.; Müller, L.; Niess, U. M.; Marahiel, M. A. Role of the Bacillus subtilis Fatty Acid Desaturase in Membrane Adaptation during Cold Shock. *Mol. Microbiol.* **2001**, *39* (5), 1321–1329. https://doi.org/10.1046/j.1365-2958.2001.02322.x

63. Chan, Y.-H. M.; Boxer, S. G. Model Membrane Systems and Their Applications State of the Field. *Curr. Opin. Chem. Biol.* **2007**, *11* (6), 581–587. https://doi.org/10.1016/j.cbpa.2007.09.020

64. Chan, Y.-H. M.; Boxer, S. G. Model Membrane Systems and Their Applications State of the Field. *Curr. Opin. Chem. Biol.* **2007**, *11* (6), 581–587. https://doi.org/10.1016/j.cbpa.2007.09.020

65. Alam, S.; Mattern-schain, S. I.; Best, M. Targeting and Triggered Release Using Lipid-Based Supramolecular Assemblies as Medicinal Nanocarriers. In *Comprehensive Supramolecular Chemistry II*; Gokel, G. W., Atwood, J. L., Eds.; Elsevier Ltd, **2017**; Vol. 5, pp 329–364. https://doi.org/10.1016/B978-0-12-409547-2.12540-5

66. Li, J.; Wang, X.; Zhang, T.; Wang, C.; Huang, Z.; Luo, X.; Deng, Y. A Review on Phospholipids and Their Main Applications in Drug Delivery Systems. *Asian J. Pharm. Sci.* **2015**, *10* (2), 81–98. https://doi.org/10.1016/j.ajps.2014.09.004

67. Akbarzadeh, A.; Rezaei-Sadabady, R.; Davaran, S.; Joo, S. W.; Zarghami, N.; Hanifehpour, Y.; Samiei, M.; Kouhi, M.; Nejati-Koshki, K. Liposome: Classification, Preparation, and

Applications. *Nanoscale Res. Lett.* **2013**, *8* (1), 1–9. https://doi.org/10.1186/1556-276X-8-102

68. Zhao, H.; Lappalainen, P. A Simple Guide to Biochemical Approaches for Analyzing Protein-Lipid Interactions. *Mol. Biol. Cell* **2012**, *23* (15), 2823–2830. https://doi.org/10.1091/mbc.E11-07-0645

69. Virtanen, J.; Brotherus, J.; Renkonen, O.; Kates, M. Synthesis of Monoacid 2,3.diacyl-*sn*-glycerols via 1,6-Ditrityl-D-Mannitol. *Chem. Phys. Lipids* **1980**, *27* (6100), 4–8. https://doi.org/10.1016/0009-3084(80)90034-1

70. Gagnon, M. C.; Dautrey, S.; Bertrand, X.; Auger, M.; Paquin, J. F. A Flexible Synthetic Approach to Phosphatidylglycerols. *European J. Org. Chem.* **2017**, *2017* (43), 6401–6407. https://doi.org/10.1002/ejoc.201701178

71. Lindberg, J.; Ekeroth, J.; Konradsson, P. Efficient Synthesis of Phospholipids from Glycidyl Phosphates. *J. Org. Chem.* **2002**, *67* (1), 194–199. https://doi.org/10.1021/jo010734+

72. Makita A.; Yamada. Y.; and Okada. H. The Total Synthesis of (±)−Patutolide A. *J. Antibiot. (Tokyo).* **1986**, *39* (9), 1257. https://doi.org/10.7164/antibiotics.39.1257

73. Lewis, A. R.; Reber, K. P. Synthesis of Antifungal Alatanone and Trineurone Polyketides. *Tetrahedron Lett.* **2016**, *57* (10), 1083–1086. https://doi.org/10.1016/j.tetlet.2016.01.090

74. Baer, T. A.; Carney, R. L. Copper Catalyzed Reaction of Grignard Reagents. *J. Chem. Inf. Model.* **2019**, *53* (9), 1689–1699. https://doi.org/10.1017/CBO9781107415324.004

75. Richardson, M. B.; Williams, S. J. Supporting Information for A Practical Synthesis of Long-Chain Iso-Fatty Acids (Iso-C_{12}-C_{19}) and Related Natural Products. *Beilstein J. Org. Chem.* **2013**, *9*, 1807–1812. https://doi.org/10.3762/bjoc.9.210

76. Kruizinga, W. H.; Strijtveen, B.; Kellogg, R. M. Cesium Carboxylates in Dimethylformamide. Reagents for Introduction of Hydroxyl Groups by Nucleophilic Substitution and for Inversion of Configuration of Secondary Alcohols. *J. Org. Chem.* **1981**, *46* (21), 4321–4323. https://doi.org/10.1021/jo00334a055

77. Seyferth, D. The Grignard Reagents. *Organometallics* **2009**, *28* (6), 1598–1605. https://doi.org/10.1021/om900088z

78. Ho, T.-L.; Fieser, M.; Fieser, L. Dilithium Tetrachlorocuprate(II). *Fieser Fieser's Reagents Org. Synth.* **2006**, No. II, 8–10. https://doi.org/10.1002/9780471264194.fos04169

79. Russell, M. A.; Laws, A. P.; Atherton, J. H.; Page, M. I. The Mechanism of the Phosphoramidite Synthesis of Polynucleotides. *Org. Biomol. Chem.* **2008**, *6* (18), 3270–3275. https://doi.org/10.1039/b808999j

80. Harbison, G. S.; Griffin, R. G. Improved Method for the Synthesis of Phosphatidylcholines. *J. Lipid Res.* **1984**, *25* (10), 1140–1142. https://doi.org/10.1016/s0022-2275(20)37724-5

APPENDICES

Appendix A1: Emission Spectra of Laurdan in POPC Vesicles

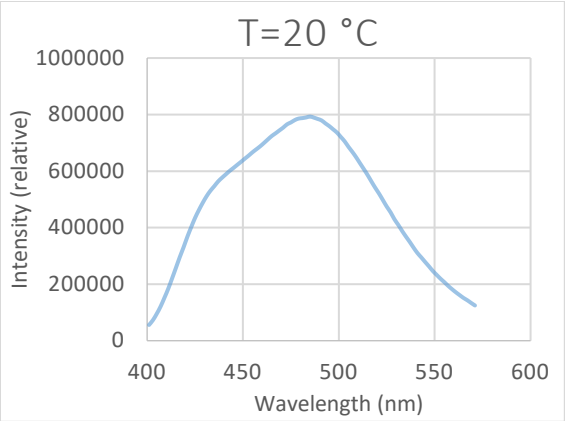

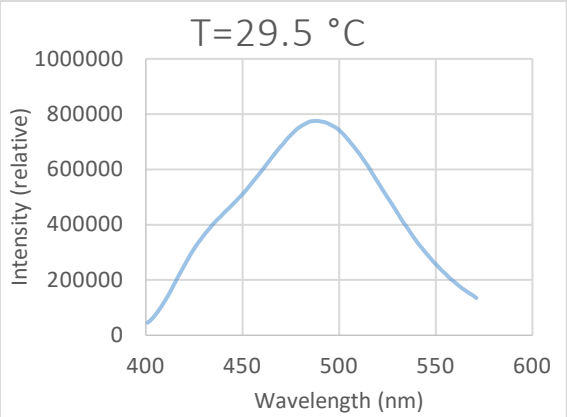

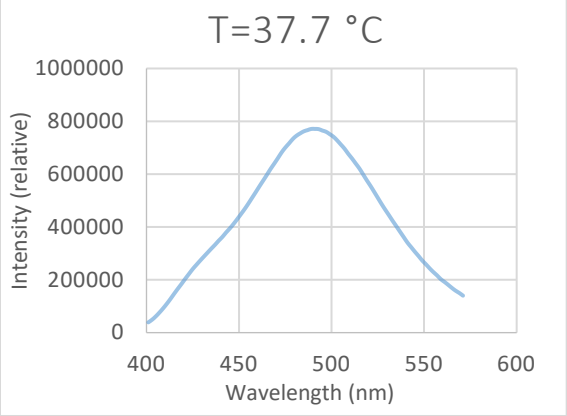

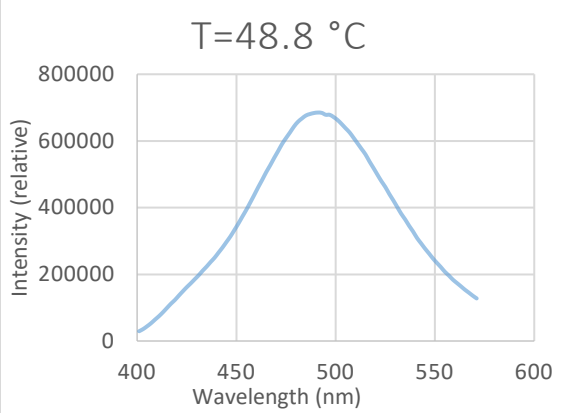

Appendix B1: GC/MS Total Ion Chromatogram of 14-Methylpentadecanoic Acid (i-16:0) Methyl Ester

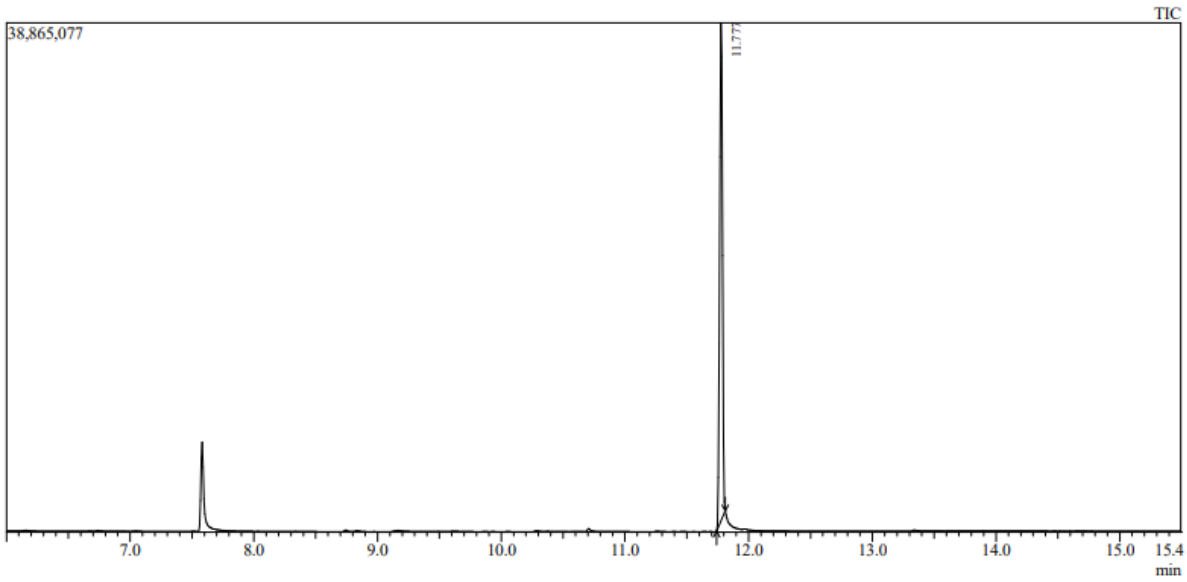

Appendix B2: Table of Gas Chromatographic Peaks for 14-Methylpentadecanoic Acid (i-:16:0) Methyl Ester

Peak No	Ret. time	Start time	End time	M/Z	Area	Area %	Height	Height %	A/H
1	7.583	7.554	7.687	TIC	1900860	10.73	11617487	17.39	1.64
2	11.80	11.733	11.936	TIC	155533293	87.87	53556658	80.17	2.90

Appendix B3: ^{1}H NMR Spectrum of 14-Methylpentadecanoic Acid (i-16:0) Before Recrystallization

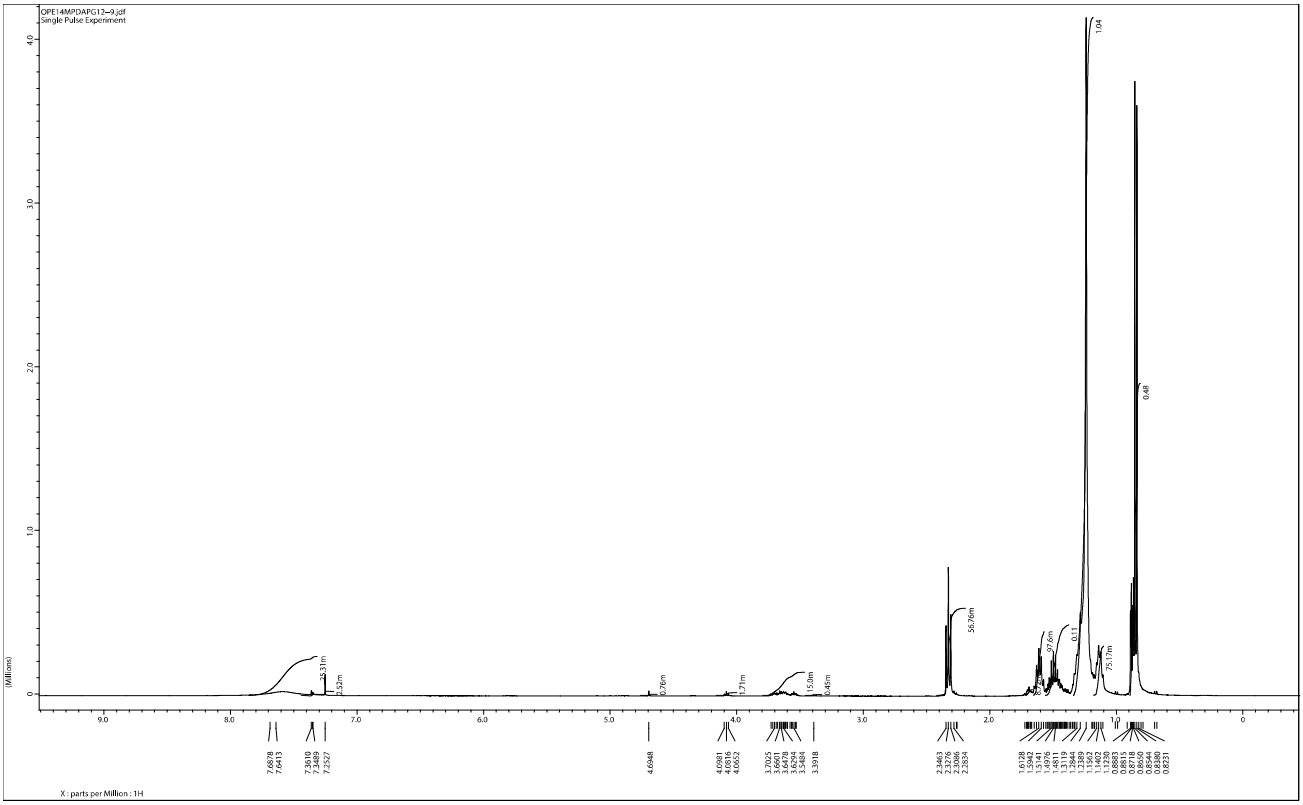

Appendix B4: ^{1}H NMR Spectrum of 14-Methylpentadecanoic Acid (i-16:0) After Recrystallization

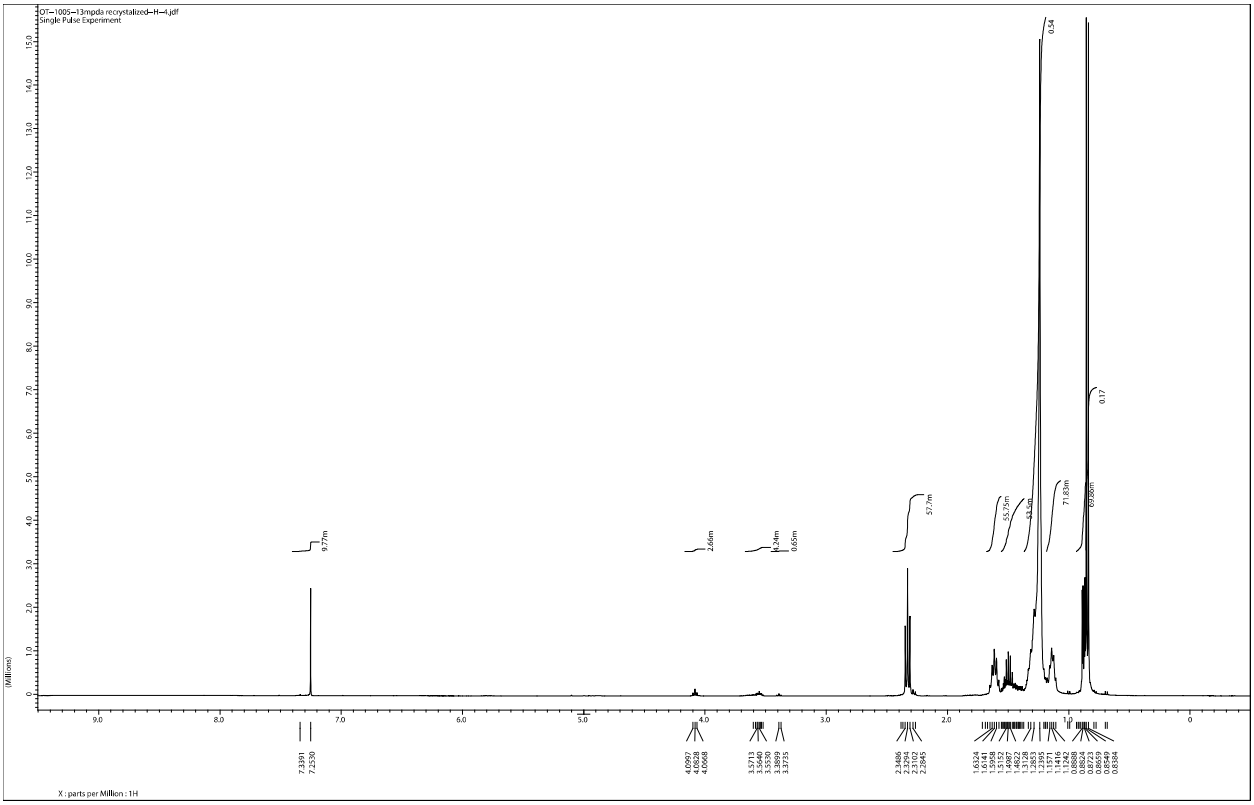

Appendix C1: ^{1}H NMR Spectrum of 13-Methyltetradecanoic Acid (i-15:0) Before Recrystallization

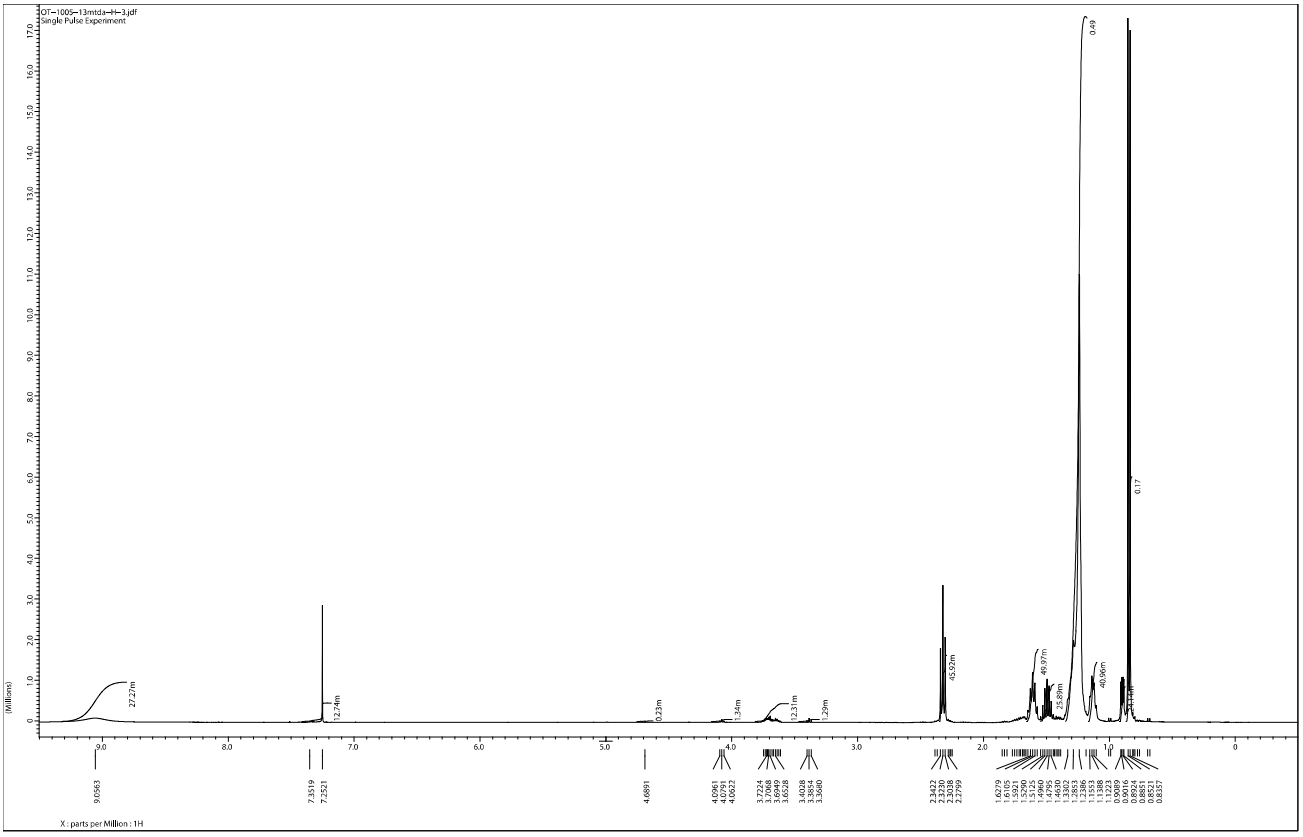

*Appendix D1: ^{1}H NMR Spectrum of Crude Phosphate Ester **6***

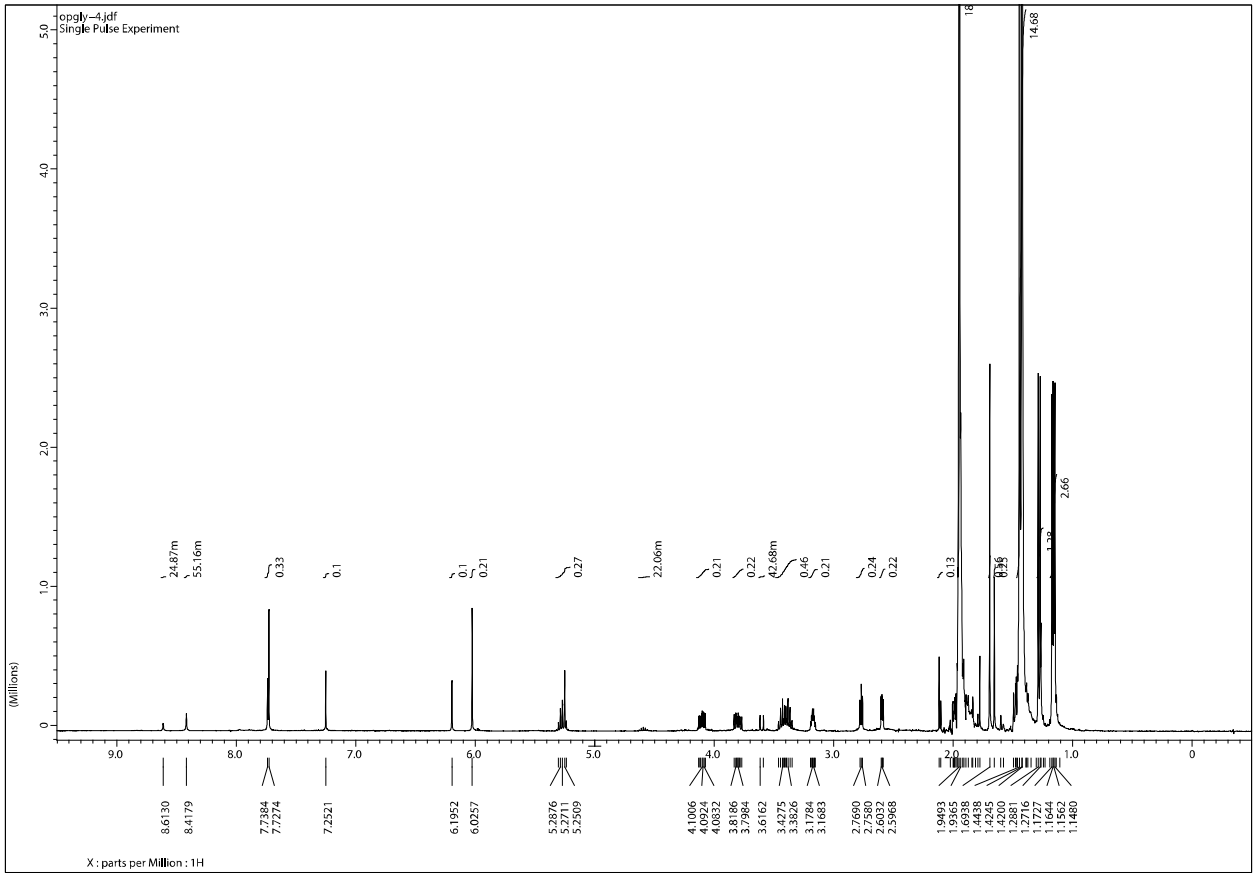

VITA

OPEYEMI TADE

Education:	B.Tech. Pure and Applied Chemistry, Ladoke Akintola University of Technology, Ogbomoso, Oyo State, Nigeria, 2014 M.S. Chemistry, East Tennessee State University, Johnson City, Tennessee, 2021
Professional Experience:	Internship, National Horticultural Research Institute (NIHORT), Ibadan,Oyo State, Nigeria, May 2012 – Oct 2012 Graduate Assistant, East Tennessee State University, College of Arts and Sciences, 2019–2021
Honors and Awards:	Miss Margaret Sells Chemistry Scholarship, Department of Chemistry. East Tennessee State University. 2021 Member of the American Chemical Society, 2019 to present
Presentation:	Three Minute Thesis (3MT), East Tennessee State University, Johnson City, TN. Oct. 15, 2020 Membranes: protecting the cell from multiple threats